PETROLOGY AND GEOCHEMISTRY OF KNOBBY PERIDOTITE ZONES WITHIN ULTRAMAFIC FLOWS AT PYKE'S HILL, MUNRO TOWNSHIP, ONTARIO

PETROLOGY AND GEOCHEMISTRY OF KNOBBY PERIDOTITE ZONES WITHIN ULTRAMAFIC FLOWS AT PYKE'S HILL, MUNRO TOWNSHIP, ONTARIO

By

DEAN W. A. MCDONALD

Submitted to the Department of Geology
in Partial Fulfilment of the Requirements
for the Degree
Bachelor of Science

McMaster University
April, 1981

BACHELOR OF SCIENCE (1981)
(Geology)

MCMASTER UNIVERSITY
Hamilton, Ontario

TITLE: Petrology and Geochemistry of Knobby Peridotite Zones Within Ultramafic Flows at Pyke's Hill, Munro Township, Ontario

AUTHOR: Dean W. A. McDonald

SUPERVISOR: Dr. James H. Crocket

NUMBER OF PAGES: 76

SCOPE AND CONTENTS:

Knobby peridotite forms a distinctive zone within the cumulus member of spinifex and non-spinifex bearing ultramafic komatiitic flows. Detailed measurements of flows at Pyke's Hill indicate the relative abundance and spatial relationships of knobby peridotites within specific types of flows. Petrographic and geochemical analysis (including whole rock, rare earth and neutron activation) have been implemented and discussed in terms of a comparison to analysis of other zones within the flow. Polished sections indicate relationships between silicate and opaque mineralogy.

ABSTRACT

Pyke's Hill provides a well preserved exposure of ultramafic komatiitic flows containing both spinifex and non-spinifex bearing end members.

Fractional crystallization and gravitational settling of olivine phenocrysts during the eruption of the magma, produce a cumulus zone with an overlying zone devoid of crystals. Quench cooling of the crystal free zone produces a spinifex textured zone above the cumulus layer.

Knobby peridotites within the cumulus portion of the flow form bands or pockets that are confined to the lower meter of the flow regardless of the thickness of the flow. Quench cooling of devitrified glass found between the olivine clusters produce the ovoid shaped knobby protuberances observed in the knobby peridotite zone.

Chemical analysis indicates only minor deviations in compositions between the different zones in the peridotite flow. Gold concentrations in the knobby peridotite and adjacent zones are low (eg. knobby peridotite contains 2.0 $\pm$ 1.0 ppb) and seem to show little variation in mildly to extensively altered flows.

The knobby peridotite zone is considered to be the most representative of the original magma since other zones show contamination by seawater cooling and/or cumulus olivine.

ACKNOWLEDGEMENTS

I would like to thank Dr. J.H. Crocket who suggested this topic and provided astute suggestions throughout the development of the thesis.

Assistance provided by Mr. A. Kabir during the neutron activation procedure was greatly appreciated. His ability to rectify a novice's mistakes is held in particular esteem.

The noteworthy talents of Mr. L. Zwicker in the preparation of thin sections; Mr. O. Murdock in chemical analysis and Mr. J. Whorwood in photography are recognized and appreciated.

Special thanks goes to Mr. J. Homosits of Selco Mining Inc. for his help and useful advice during the drafting of figures. Gwen-Ella McDonald's significant typing skills will be viewed in the following pages.

An NSERC Grant to Dr. Crocket supplies partial financial assistance, for which I am very appreciated.

TABLE OF CONTENTS

LIST OF TABLES

LIST OF PLATES

LIST OF FIGURES

CHAPTER 1

Introduction and Background

1.1 Introduction

Since the generation of ultramafic peridotite magmas require temperatures of 1500 - 1600^{o}C (Vogt, 1926), duplication under present surface conditions is impossible. Due to advancements in igneous petrology, scientists have recently acknowledged the probability of extrusive magma rock.

Bowen's (1956) early objection to the formation of ultramafic rocks involved the excessively high melting temperature necessary for the re-solution of olivine to give peridotite liquid. The failure of inclusions of rock within peridotite to show contact aureoles or other alteration effects seemed to contradict the high temperature hypothesis.

Work by Green and Ringwood (1967), Green (1975) indicated that during the Archean, the lowering of the geothermal gradient along with degassing of the mantle would allow for partial melting of the upper mantle to produce liquids of peridotite composition. Older Archean belts (Kaapval Craton in South Africa; Western Australian Shield) maintained a lower geothermal gradient during formation than younger belts (Canadian Shield) producing greater concentrations of ultramafic rocks.

The association of nickel sulfide deposits with peridotite lava flows in Western Australia (Woodal and Travis, 1969), the Manitoba nickel belt and the Ungava nickel belt (Naldrett and Cabri, 1976) have stimulated significant study and exploration for deposits of this type.

Due to the excellent preservation of peridotite lava flows at Pyke's Hill in Munro Township, Ontario, detailed study of individual ultramafic flows are possible. Individual ultramafic flows usually consist of two major units; an upper spinifex textured zone containing long parallel needles of olivine and a lower cumulus zone containing moderately foliated peridotites. This spinifex bearing flow is the end member of a continuum that ranges from flows with large spinifex textured portions to flows devoid of spinifex textures.

Within the cumulus portion of some flows is a band characterized by a weathering surface of knobby or oval shaped areas that stand out in positive relief. The presence of knobby peridotite is not widespread in Munro Township flows (Arndt et al, 1977) and is poorly mapped. The origin and genetic significance of knobby peridotites has not been extensively studied and is still not completely understood. The purpose of this thesis is to investigate the occurrence of knobby peridotites within the extrusive ultramafic flows of Pyke's Hill and comment on their origin, distribution and individual composition.

1.2 Previous Work

a) Ultramafic Rocks

Naldrett and Mason (1968), working in the Dundonald and Clergue Township in Ontario, demonstrated that volcanic rocks of ultramafic composition formed an integral part of the volcanic stratigraphy. The presence of pillowed structures in peridotite lavas on the Barberton Mountainland in South Africa (Viljoen and Viljoen, 1969) provide evidence for extrusive subaqueous volcanism. Work by Nesbitt (1971) on the Yilgarn Block of Western Australia recognized skeletal olivine textures in "spinifex rock" and interpreted this texture as the product of rapid growth in a supercooled liquid. The spinifex texture forms by an in situ crystallization in a crystal-free ultramafic liquid. Pyke et al (1973) outlined a number of features of flows at Pyke's Hill that implied an extrusive origin. Previous work had interpreted these flows as intrusive rock (Berry, 1940) and classified them as peridotites (Satterley, 1952; MacRae, 1965).

Recent study by Arndt et al (1977) suggests that komatiitic lavas in Munro Township form a succession that is both underlain and overlain by thicker sequences of tholeiitic volcanic rocks. A broader definition of komatiites was proposed by Arndt et al (1977) to include all members of this ultramafic series.

b) Munro Township

A detailed study of Munro Township and adjacent areas was produced by Satterley and Armstrong (1947) with subsequent work by Satterley (1951). Although reinterpretation of rock suites has occured (MacRae, 1965; Pyke et al, 1973; Arndt et al, 1977); this work still serves as an excellent reference. The geology of Munro Township was also included in Goodwin and Ridler's (1969) treatment of the Abitibi greenstone belt.

Many of the differentiated sills in the area have been studied and presented in various theses and publications. MacRae (1963) wrote a

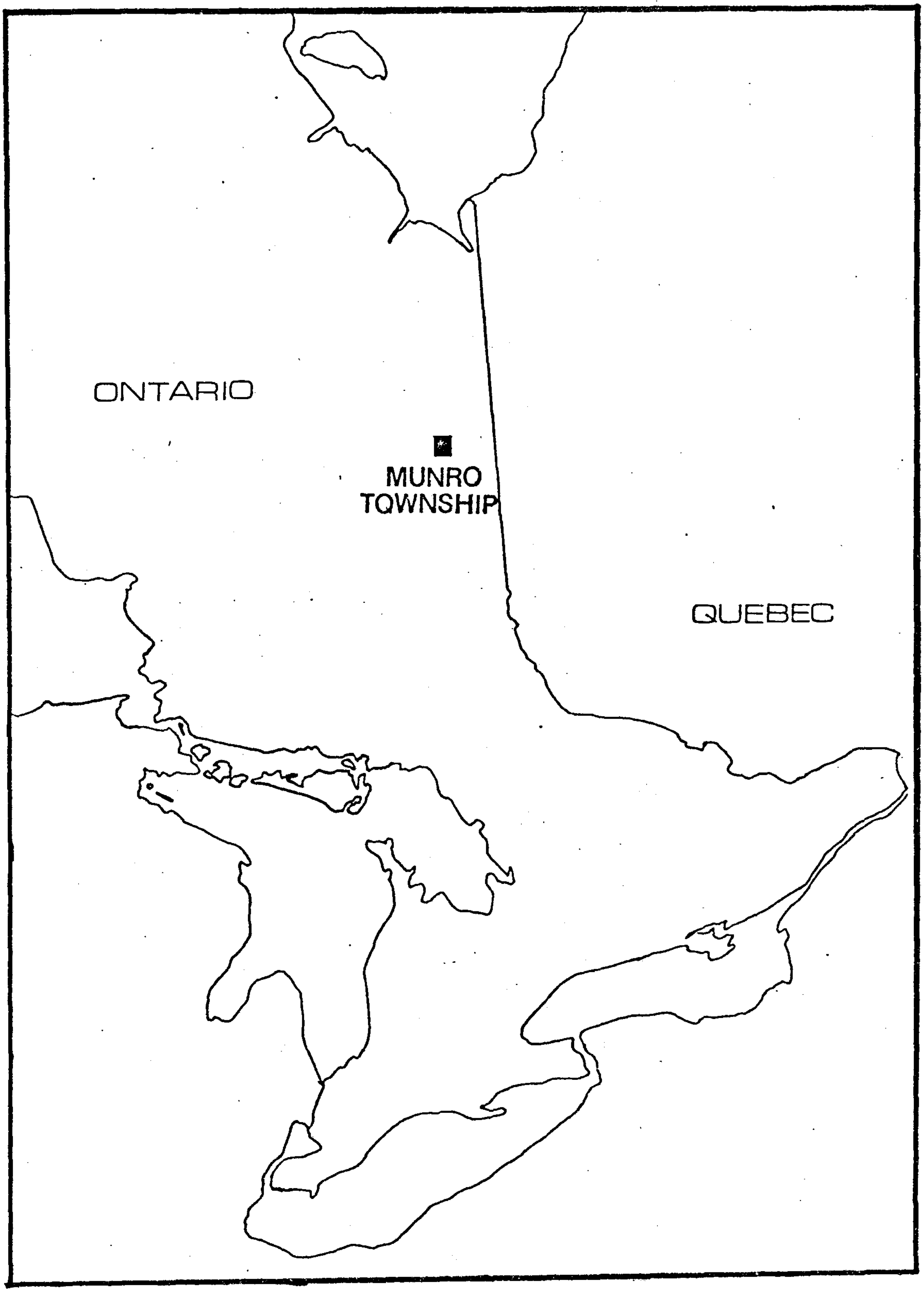

FIGURE 1

Location Map

FIGURE 2

Map of Munro Township showing location of study area (PYKE'S HILL) relative to transportation routes and prominent geographic features.

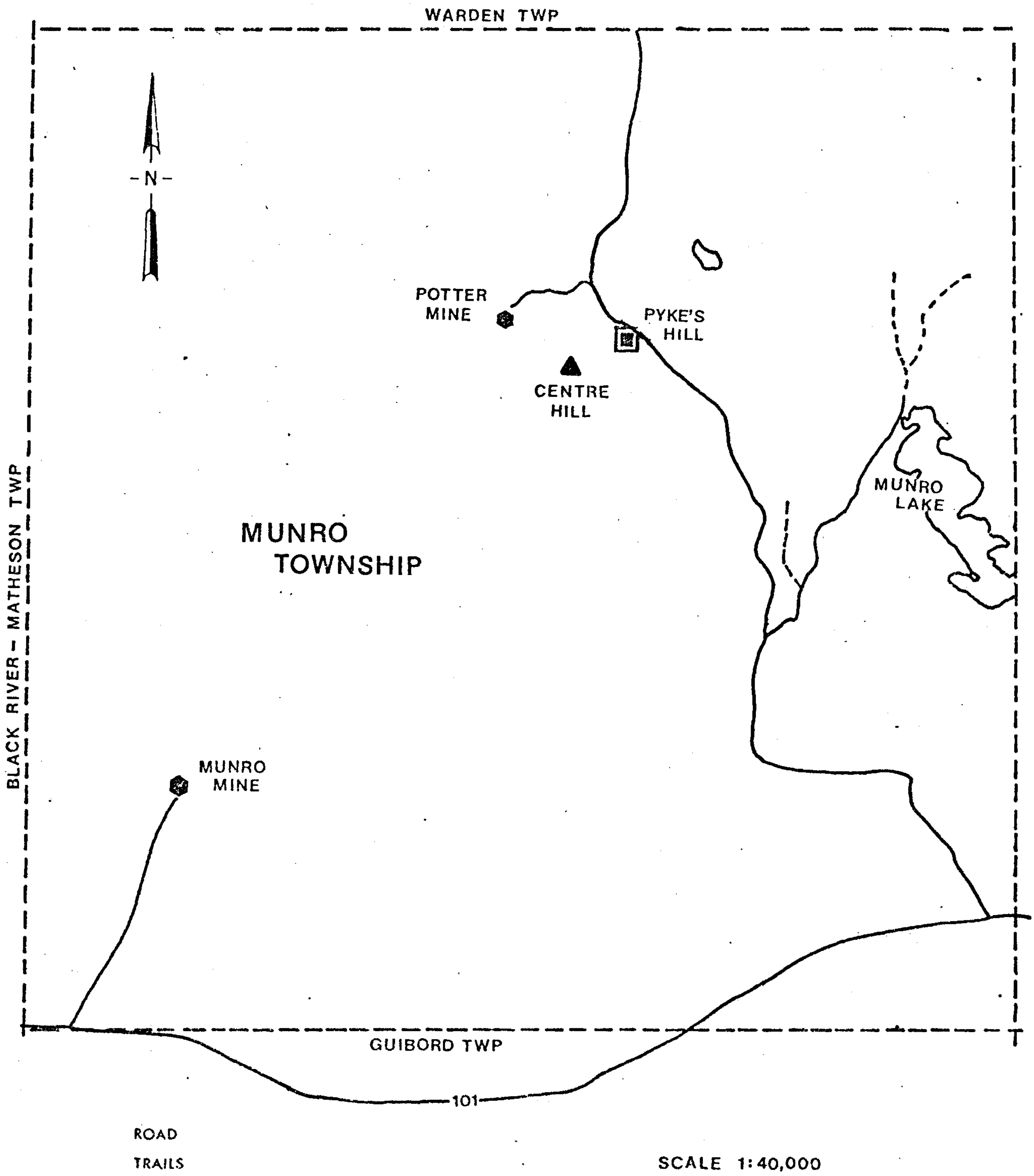
WARDEN TWP
N
POTTER
MINE
PYKE'S
HILL
CENTRE
HILL
MUNRO
LAKE
MUNRO
TOWNSHIP
BLACK RIVER - MATHESON TWP
MUNRO
MINE
GUIBORD TWP
101
ROAD
TRAILS
SCALE 1:40,000

thesis on the Centre Hill Complex and then expanded his study to include a number of sills in the region. (MacRae, 1965, 1969). Naldrett and Mason (1968) studied the Dundonald sill and associated ultramafic rocks in the Clergue and Dundonald Townships.

The initial recognition of peridotite flows in Munro Township was reported by Pyke et al (1973) and later treated by Arndt (Arndt, 1975; Arndt et al, 1977)

1.3 Location and Accessibility

Munro Township lies south of Lake Abitibi and about 80 kilometers east of Timmins in northeastern Ontario (Figure 1). The study area is located in the central portion of Munro Township adjacent to the Potter Mine property (Figure 2). A gravel road to the Potter Mine cuts by Pyke's Hill and allows easy access to the outcrop by foot. This gravel road is connected to Highway 101, the main highway route to Timmins in the west and Noranda to the east.

1.4 Regional Geology

The east trending Abitibi Belt has been described by Goodwin and Ridler (1970) as a crudely S-shaped belt 800 kilometers long by 90 - 160 kilometers wide. The belt is bound west and east by northeast trending gneissic rocks of the Kapuskasing subprovince and the Grenville structural province respectively (Figure 3).

A major portion of the greenstone belt consists of thin (2 meters to 20 meters thick) pillowed and massive flows of ultramafic composition.

These flows are interlayered with thick (100 meters to 200 meters thick) differentiated sills that typically comprise of a basal zone of peridotite, transitional upwards through pyroxenitic gabbro to gabbro or pyroclastic rocks (Goodwin and Ridler, 1970). Granitic and syenite plutons generated during the Kenoran orogeny randomly cut into the volcanic sequences (Jolly, 1980).

Munro Township lies within the Abitibi greenstone belt and consists predominantly of ultramafic komatiitic and mafic lavas.(Arndt et al, 1977). Arndt et al, (1977) have proposed a generalized volcanic sequence that indicates cyclic variations starting with thin ultramafic flows and ending with thicker mafic flows. The composition of the lava flows become more mafic with increasing stratigraphic height. Thin but persistent bands of siliceous tuff and chert are intercalated with the volcanic rocks. Small peridotite sills and dykes or large layered peridotite gabbro sills intrude the volcanics and sediments (Arndt et al, 1977).

1.5 Metamorphism

The eruption of mafic and ultramafic volcanics on the gneissic complex produced downwarping and block faulting. During and soon after eruption of volcanics a regional prehnite - pumpellyte grade was superimposed on permeable parts of the pile due to burial metamorphism (Jolly, 1980).

All petrographic evidence (Jolly, 1980, Arndt et al, 1977) indicates that Pyke's Hill and surrounding area has retained the prehnite - pumpellyte grade of metamorphism.

FIGURE 3

Map of the Abitibi orogenic belt (after Goodwin and Ridler, 1970) showing the location of Munro Township, and the known distribution of rocks with spinifex texture (after Eckstrand, 1972).

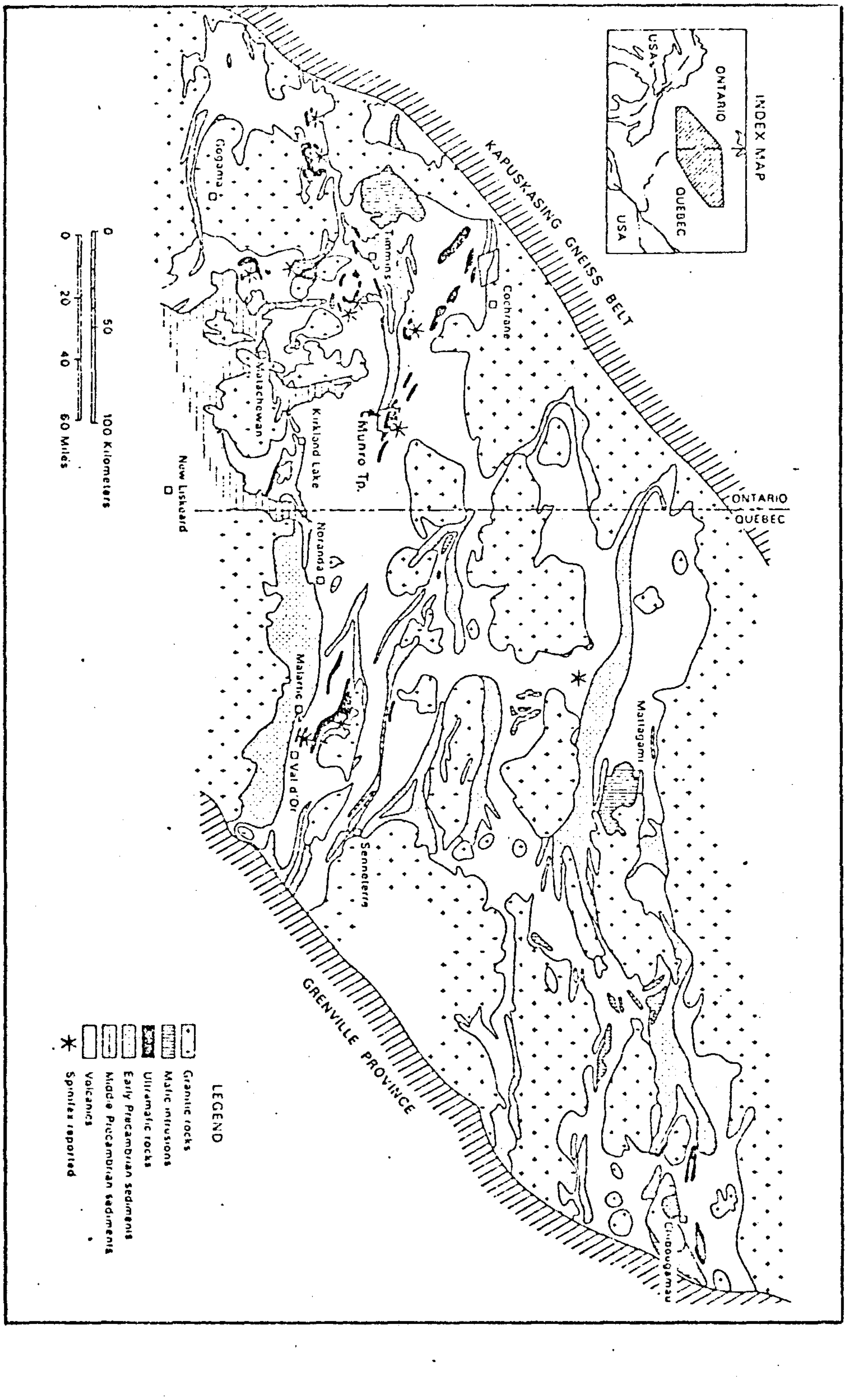
INDEX MAP
ONTARIO
QUEBEC
USA
USA
KAPUSKASING GNEISS BELT
Cochrane
Timmins
Gogama
Munro Tp.
Matachewan
Kirkland Lake
New Liskeard
ONTARIO
QUEBEC
Noranda
Malartic
Val d'Or
Senneterre
Matagami
Chibougamau
GRENVILLE PROVINCE
0 50 100 Kilometers
0 20 40 60 Miles
LEGEND
Granitic rocks
Mafic intrusions
Ultramafic rocks
Early Precambrian sediments
Middle Precambrian sediments
Volcanics
Spinifex reported

CHAPTER 2

Field Observations and Data

2.1 Sampling and Field Measurements

A series of samples numbered 1 to 17 were collected from knobby peridotite zones in flows from Pyke's Hill (Figures 4, 5, 6). Detailed mapping of area A (Figure 5) and area B (Figure 6) show spatial relationships between the textural zones of the flow and indicate sample locations. The arrows in diagram 4 signify the traverse paths used to compile detailed measurements of the flows and their specific zones. Tabulation and comparison of this data is shown in Figures 8, 9, 10.

2.2 Criteria for Komatiites

The criteria for komatiites is expressed in terms of field, petrologic and chemical features of the rock as a member of a series. Characteristics of the komatiitic series is as follows:

i) The series contains lavas that exhibit volcanic structures such as spinifex texture and polyhedral or polygonal jointing.

ii) Petrologically the series comprises of noncumulate rocks ranging in composition from peridotite (≈30 per cent MgO, 44 per cent SiO_2) to basalt 8 per cent MgO, 52 per cent SiO_2) and cumulate rocks ranging from peridotite (up to 40 per cent MgO) to mafic gabbro (≈12 per cent MgO).

FIGURE 4

Geological map of Pyke's Hill, showing ultramafic komatiitic lava flows and sample locations. Traverse lines indicate where measurements of flows were taken. (Modified from Pyke et al., 1973).

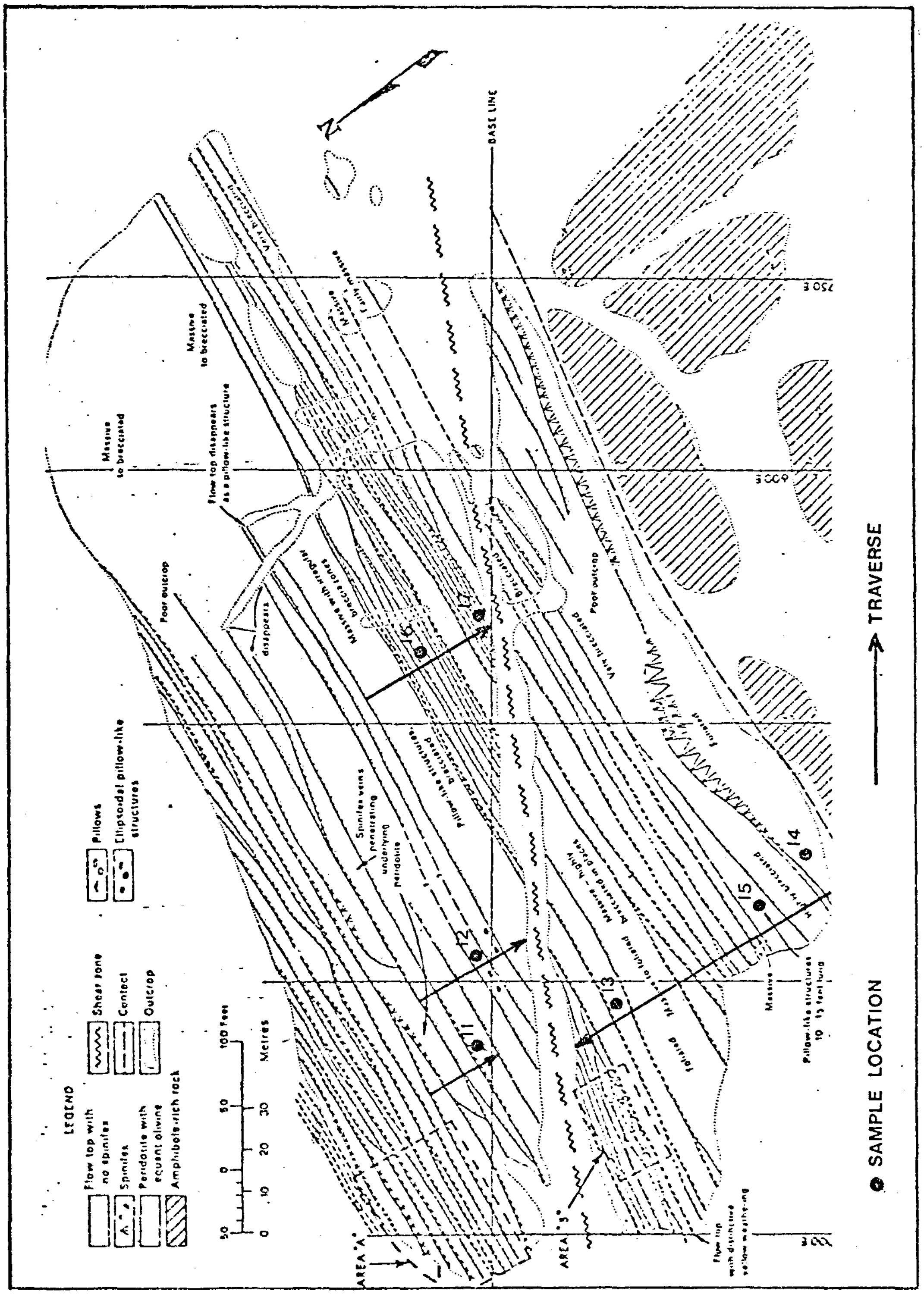
LEGEND
Flow top with no spinifex
Spinifex
Peridotite with equant olivine
Amphibole-rich rock
Shear zone
Contact
Outcrop
Pillows
Ellipsoidal pillow-like structures
Metres
100 Feet
AREA "A"
AREA "B"
BASE LINE
N
SAMPLE LOCATION
TRAVERSE
Poor outcrop
Massive to brecciated
Very brecciated
Spinifex veins penetrating underlying peridotite
Massive
Brecciated
Foliated
Sheared
11
12
13
14
15
16
17

FIGURE 5

Detailed map of Area A shown in Figure 4. Map gives spatial relationship between knobby peridotite and other zones within the komatiitic flow. Sample locations are also indicated. (Modified from Pyke et al, 1973).

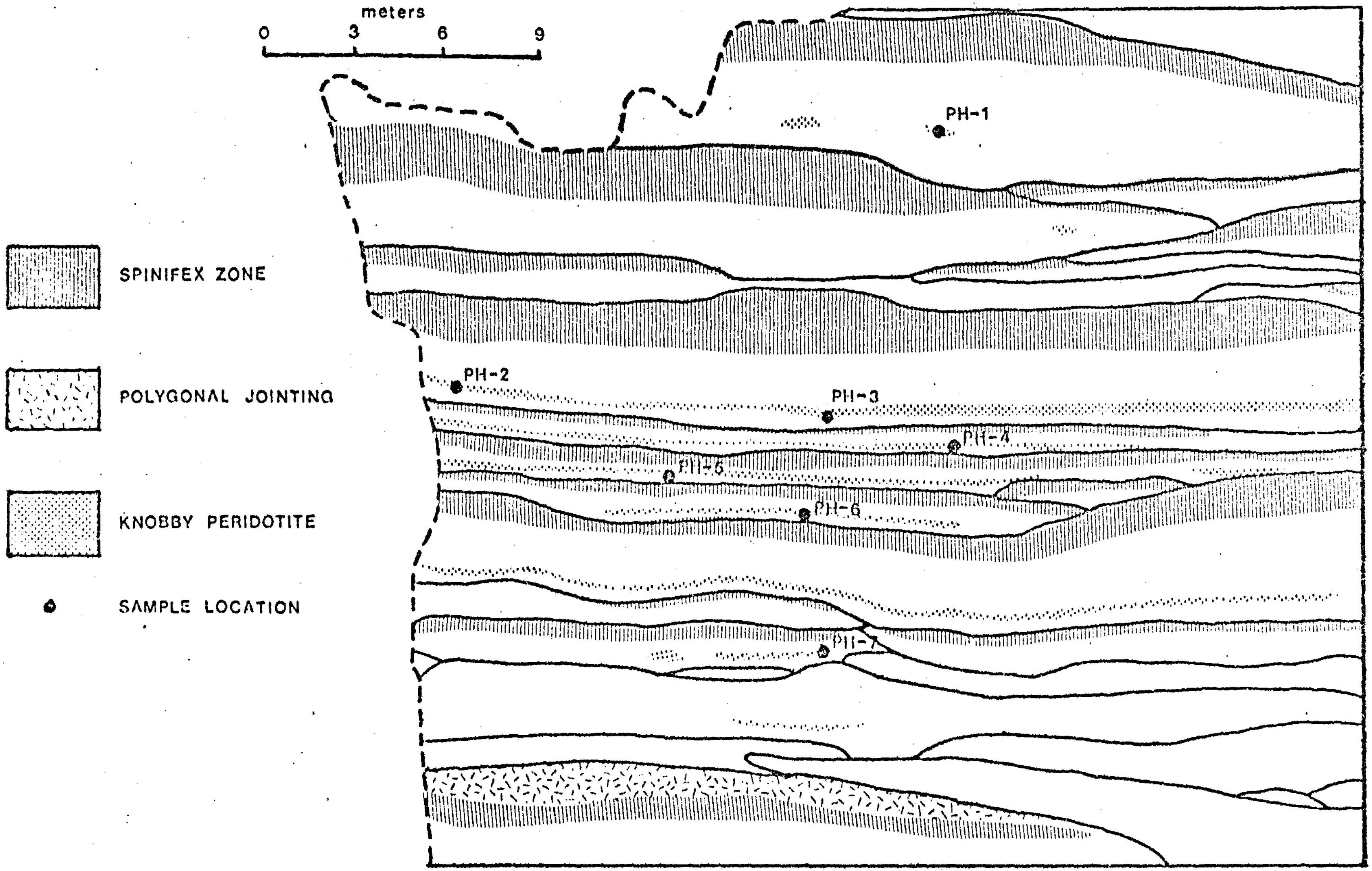
meters
0
3
6
9
SPINIFEX ZONE
POLYGONAL JOINTING
KNOBBY PERIDOTITE
SAMPLE LOCATION
PH-1
PH-2
PH-3
PH-4
PH-5
PH-6
PH-7

AREA A

FIGURE 6

Detailed map of Area B shown in Figure 4. Spatial relationship of knobby peridotite zones sample locations are indicated. (Modified from Pyke et al, 1973).

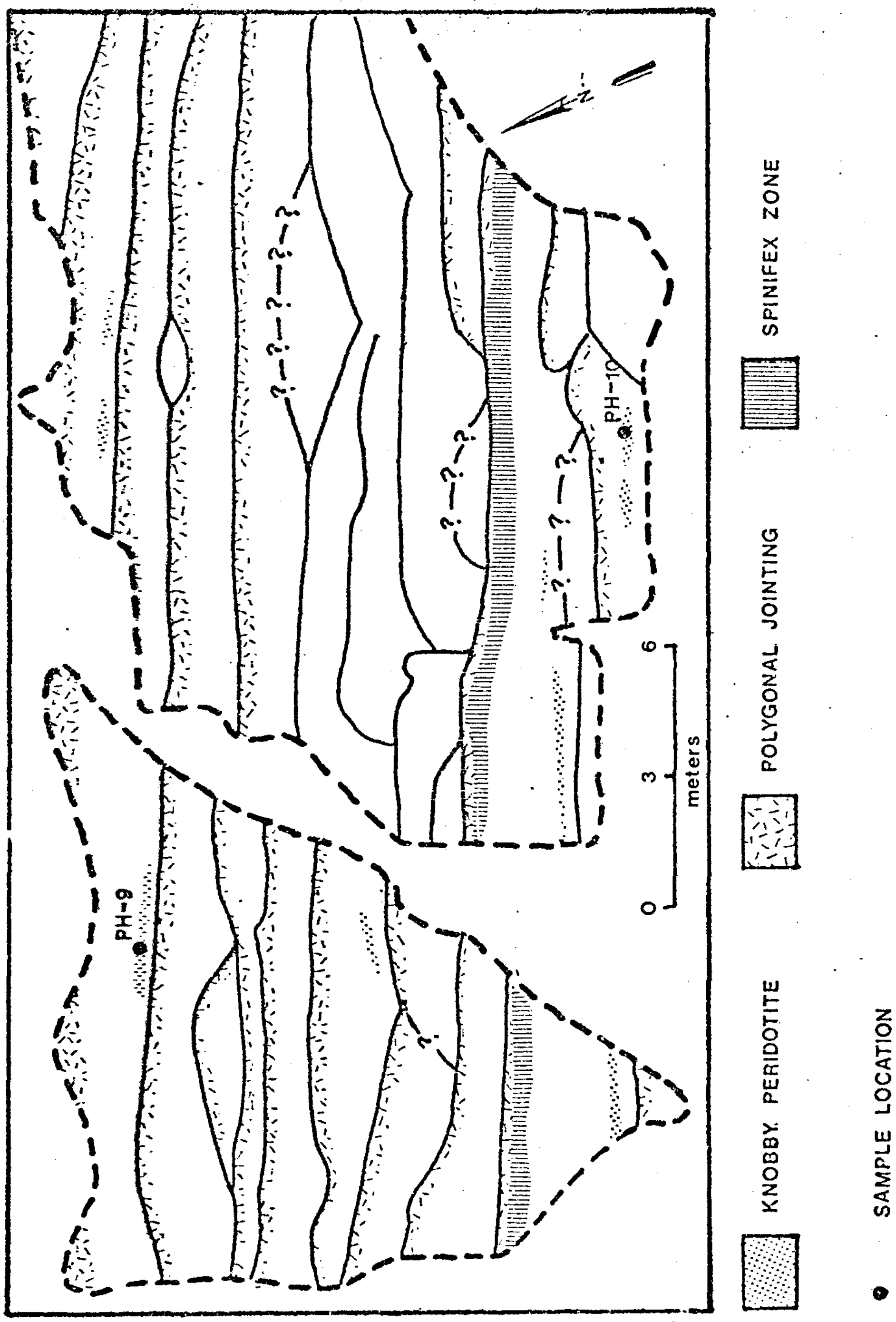
PH-9
PH-10
0
3
6
meters
KNOBBY PERIDOTITE
POLYGONAL JOINTING
SPINIFEX ZONE
SAMPLE LOCATION

AREA B

The compositions of the noncumulate rocks closely resemble the compositions of the silicate liquids from which they form.

iii) Chemically the series have low $FeO/(FeO + MgO)$ ratios, low TiO_2 contents, and high MgO, NiO, and Cr_2O_3 content, and some have high CaO/ Al_2O_3 ratios.

2.3 Spinifex Bearing Flows

The upper boundary of spinifex bearing flows is defined by a chilled margin containing closely spaced polygonal joints (Zone A_1, plate 2 and Figure 7). Some of the joints extend down into the spinifex zone which underlies the chilled margin.

The spinifex zone (A_2) contains long fine needles of olivine that grow in parallel or slightly radial patterns toward the base of the flow. Under closer inspection, these needles appear as a series of crystals stacked on one another, coarsening downward then terminating abruptly.

A narrow zone (B_1) underlying the spinifex consists of minute foliated needles of olivine oriented parallel to the flow direction. This foliated skeletal olivine was only rarely observed.

The rest of the flow consists of the cumulus zone (B_2) that exhibits a fairly homogeneous granular texture on the outcrop surface. The knobby peridotite zone (B_3) forms a band or pocket of rough, unevenly weathered modules that form protuberances in the surface. The reddish colour of the individual modules (plate 3) contrast with the grey exterior of the cumulus zone rock. The base of the flow (B_4, Figure 7) contains a

FIGURE 7

Diagramatic sections through three types of peridotite lave flows: A, a flow with an upper spinifex zone; B, a flow with limited spinifex texture; C, non spinifex bearing flow. (after Arndt _et al_., 1977).

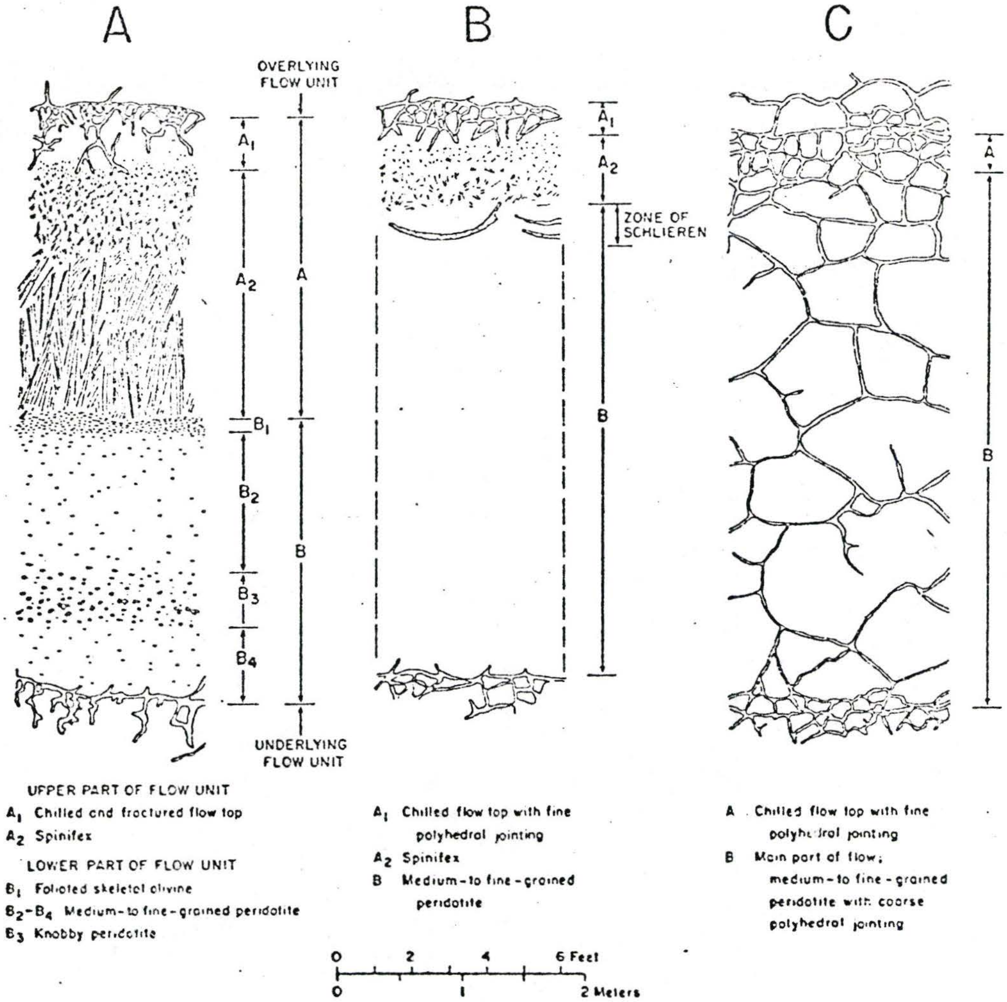
A
B
C
OVERLYING FLOW UNIT
UNDERLYING FLOW UNIT
A_1
A_2
A
B_1
B_2
B
B_3
B_4
ZONE OF SCHLIEREN
UPPER PART OF FLOW UNIT
A_1 Chilled and fractured flow top
A_2 Spinifex
LOWER PART OF FLOW UNIT
B_1 Foliated skeletal olivine
B_2–B_4 Medium- to fine-grained peridotite
B_3 Knobby peridotite
A_1 Chilled flow top with fine polyhedral jointing
A_2 Spinifex
B Medium- to fine-grained peridotite
A Chilled flow top with fine polyhedral jointing
B Main part of flow; medium- to fine-grained peridotite with coarse polyhedral jointing
0 2 4 6 Feet
0 1 2 Meters

PLATE 1

Pyke's Hill exposure viewed from the west. Dashed lines indicate margins of each flow. Location of the flow in PLATE 2 can be traced to flow (F).

PLATE 2

Individual spinifex bearing flow.

A_1 - Upper chilled margin

A_2 - Spinifex

B_1 - Foliated skeletal olivine

B_2 - Cumulus peridotite

B_3 - Knobby peridotite

Scale - pen (10 inches)

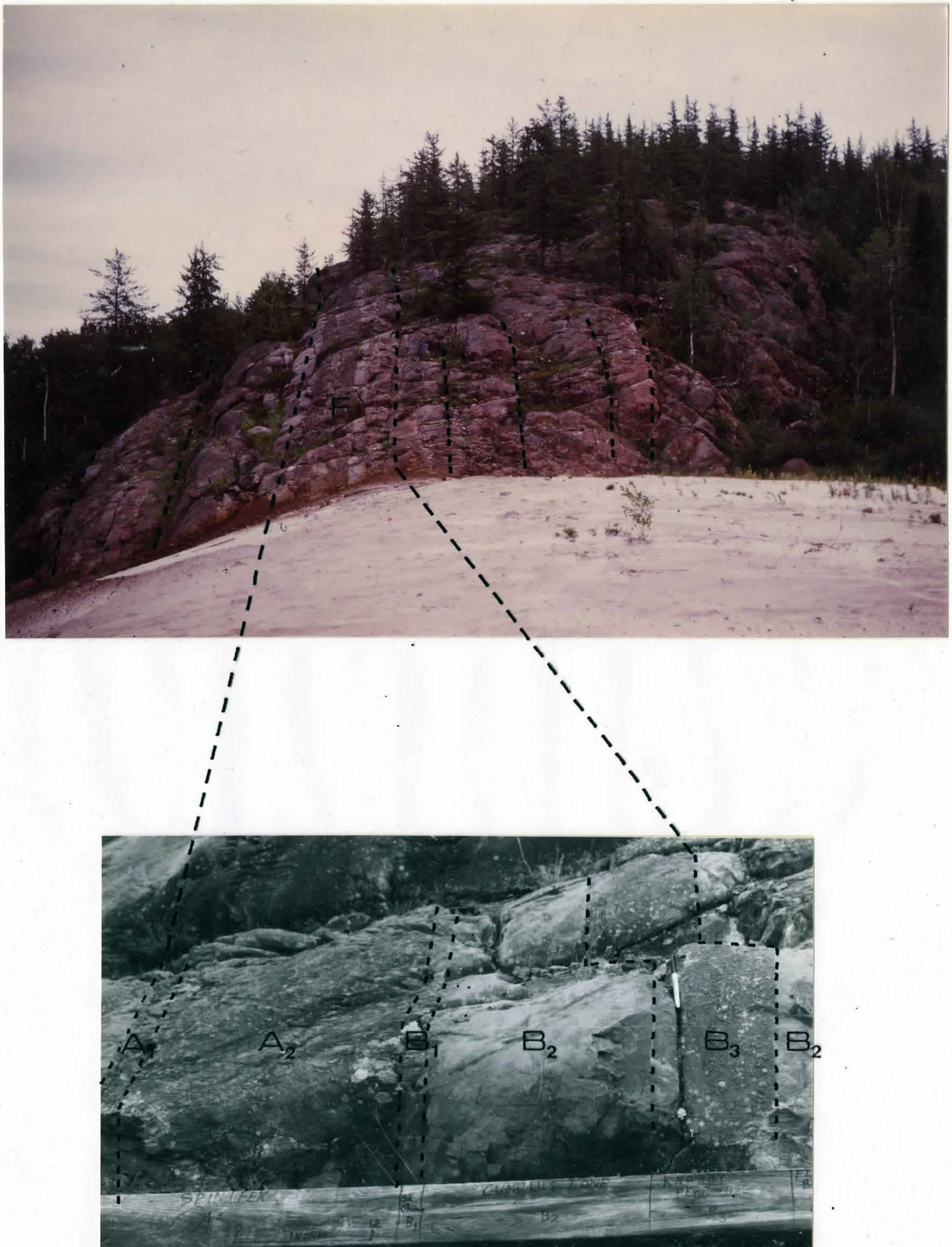
F
A_1
A_2
B_1
B_2
B_3
B_2

PLATE 3

Knobby peridotite weathering surface developed in a komatiitic flow at Pyke's Hill. Glass veinlets as well as knobby protuberances are shown.

Scale: (PEN) 10 inches.

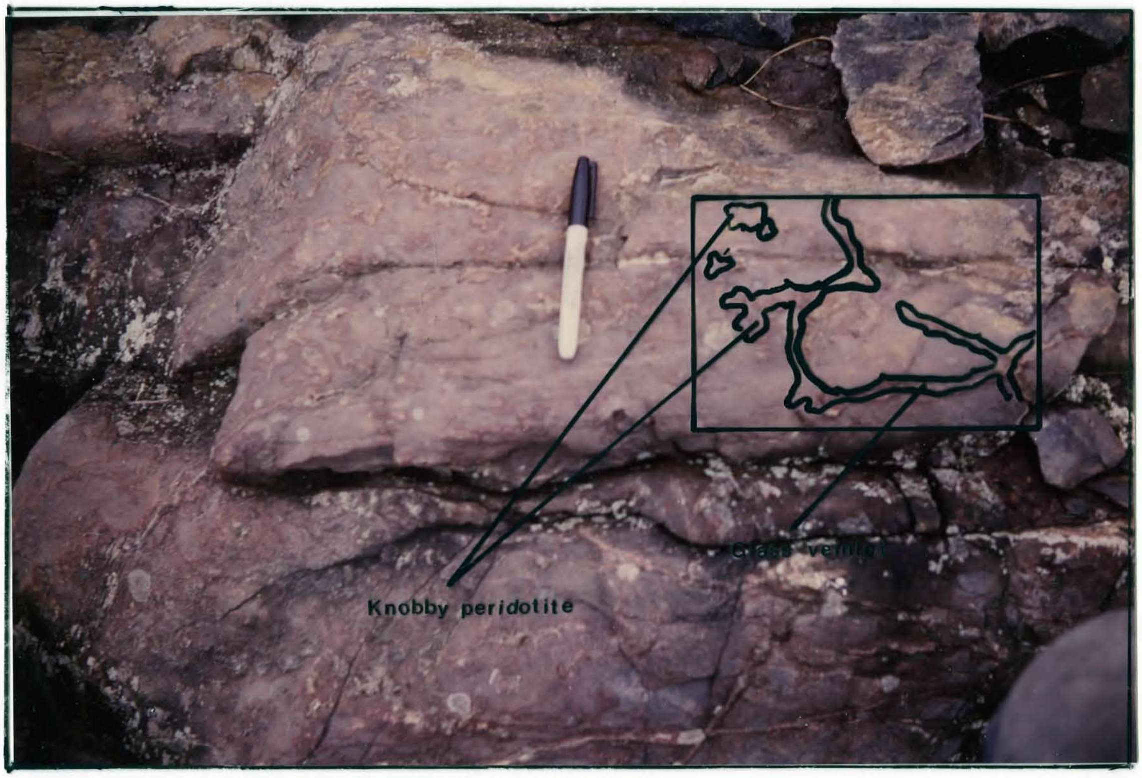
Glass veinlet
Knobby peridotite

zone of cumulus material similar to the B_2 zone. The flow base terminates against the polygonal jointing of the underlying flow.

2.4 Non-Spinifex Bearing Flows

Flows without spinifex have poorly defined textural zones (type C, Figure 7). The closely spaced polygonal joints near the upper flow margins expand into larger, well formed jointing networks that can extend to the base of the flow. Interstitial to the polygonal joints are patches of cumulus textured flow. This homogeneous texture has led to the classification of these flows as massive (Arndt *et al*, 1977), however, detailed observations show that some knobby peridotite does occur.

In those non-spinifex bearing flows with knobby peridotite, the upper zone containing polygonal jointing fades into a cumulus zone (B_3). Bands or pockets of knobby peridotite cut across this cumulus zone leaving a small section of cumulus textured rock at the base of the flow.

2.5 Others

Between the two types of flow end members of number of variants can occur. Some flows may produce only narrow zones of spinifex that pinch out, while in non-spinifex flows, polygonal jointing may not be very extensive. For convenience, all the flows were classified as one of the two end members. Those flows badly brecciated (particularly in the eastern end of the outcrop) were excluded from the data.

2.6 Knobby Peridotite Zone

The nodules producing the knobby peridotite texture are usually circular in shape and vary in size from 0.1 centimeters to 1.0 centimeters. Networks of ridged veinlets showing positive relief connect one nodule to another (plate 3). The individual nodules maintain similar morphologies in both spinifex bearing and non-spinifex bearing flows.

Knobby peridotite zones with both types of flows form stratiform bands or pockets and are both restricted to the lower meter and one half of the flow.

Knobby peridotite bands vary from 1/8 of a meter to just under one meter in width. The fluctuation of knobby peridotite band widths is minor with few bands pinching out. The distribution of individual nodules within the band is quite uniform.

Knobby peridotite pockets are elliptical in shape and usually pinch out at both ends. The long axis of the ellipsoid shaped pockets vary from less than one meter to three meters in length, while the short axis usually varies from 1/3 to one-half meters in length. Distribution of individual nodules within pockets may show random concentrations, however, no concentration trend involving nodules is evident when moving from the core of the pocket outward.

Knobby peridotite in either form occurs in just under sixty per cent of the spinifex bearing flows, and just over forty per cent of the non-spinifex bearing flows. As suggested in Figure 8, knobby peridotites are more likely to form as pockets in non-spinifex bearing flows, while bands of knobby peridotite are more common in spinifex bearing flows.

The width of spinifex zones within the flow show no correlation to the width of the knobby peridotite zone. Polygonal jointing in non-spinifex bearing flows show greater width when knobby peridotite zones are small or non-existent.

Knobby peridotite is found in a wide range of flow widths, however, flows with widths greater than four meters appear to lack knobby peridotite completely.

FIGURE 8

Percentage of flows with or without spinifex containing nodular peridotite bands or pockets. Calculated from sixty flows observed.

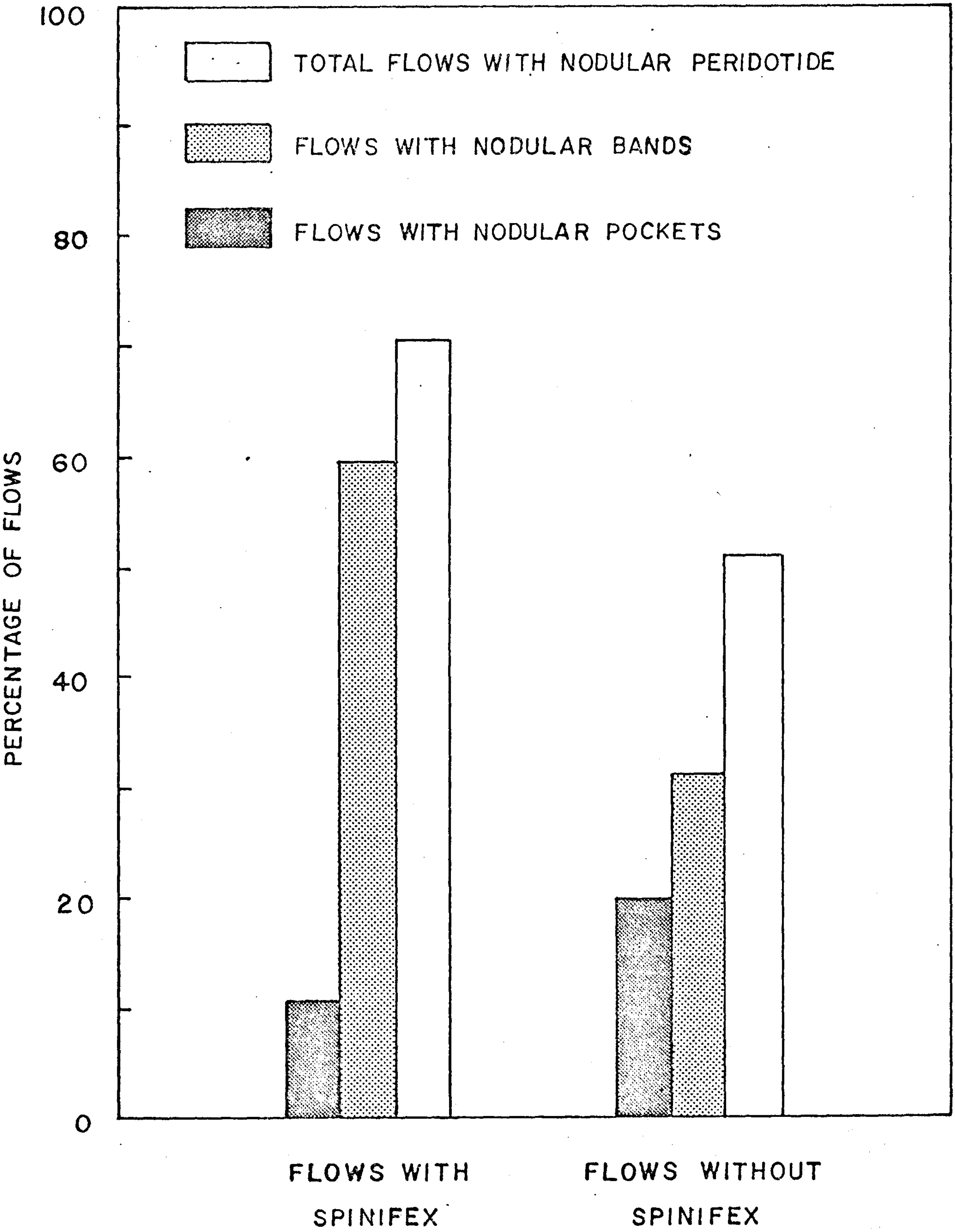
100
80
60
40
20
0
PERCENTAGE OF FLOWS
TOTAL FLOWS WITH NODULAR PERIDOTIDE
FLOWS WITH NODULAR BANDS
FLOWS WITH NODULAR POCKETS
FLOWS WITH SPINIFEX
FLOWS WITHOUT SPINIFEX

FIGURE 9

Size and spatial relationship between spinifex and knobby peridotite zones.

(Horizontal axis shows the number of flows at a specific thickness)

eg. Flow - 17 feet thickness

SPINIFEX ZONE

7 Feet thickness

KNOBBY PERIDOTITE

¼ Feet thickness

KNOBBY PERIDOTITE

1.5 Feet above the base of the flow

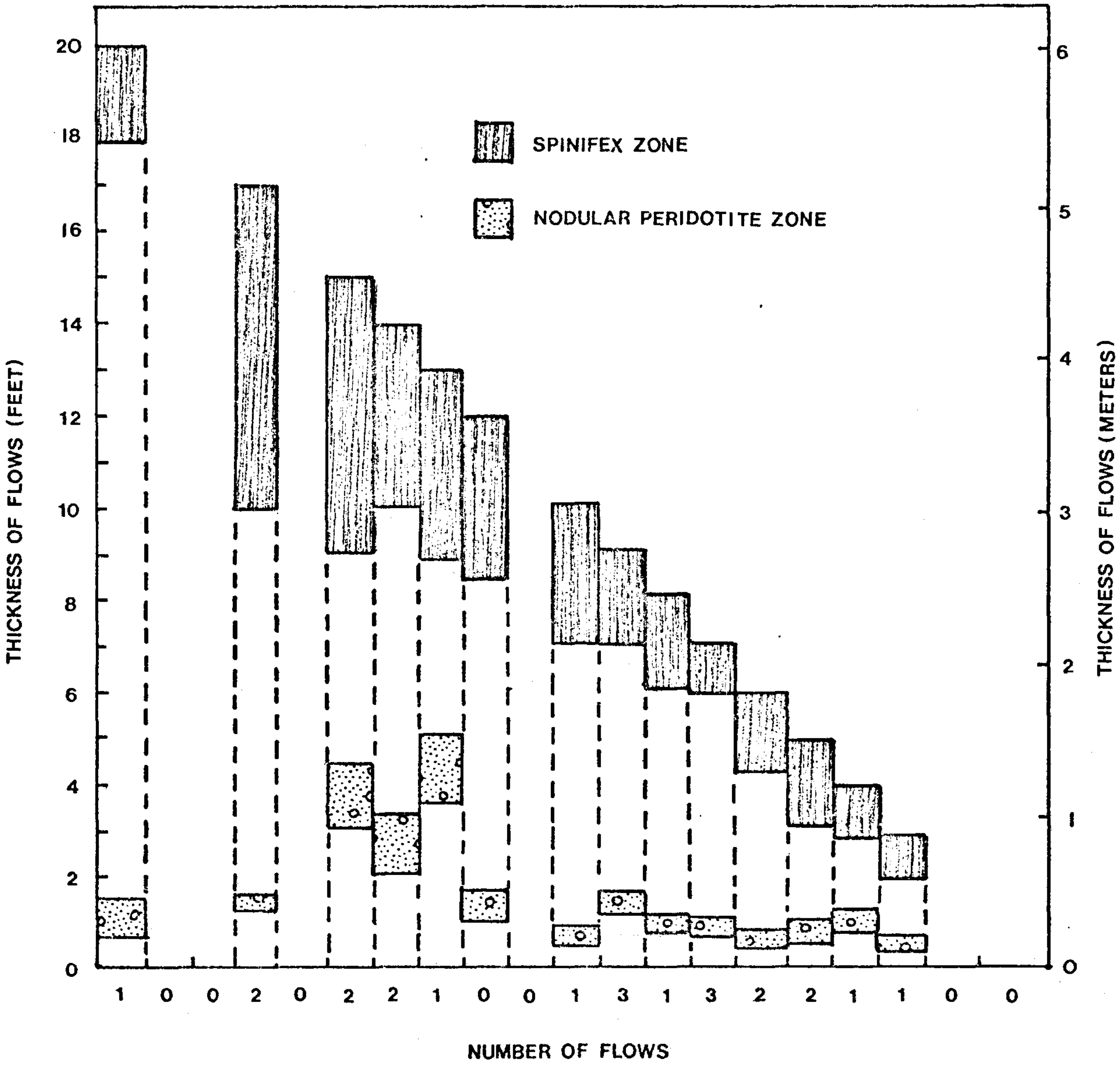
SPINIFEX ZONE
NODULAR PERIDOTITE ZONE
THICKNESS OF FLOWS (FEET)
THICKNESS OF FLOWS (METERS)
0
2
4
6
8
10
12
14
16
18
20
1
2
3
4
5
6
1 0 0 2 0 2 2 1 0 0 1 3 1 3 2 2 1 1 0 0
NUMBER OF FLOWS

FIGURE 10

Size and spatial relationship between polygonal jointing and knobby peridotite zone.

(Horizontal axis shows the number of flows at a specific thickness)

eg. Flow - 17 Feet thickness

POLYGONAL JOINTING - 6 Feet thickness

KNOBBY PERIDOTITE - 1 Foot thickness

KNOBBY PERIDOTITE - Is 0.5 feet above the base of the flow.

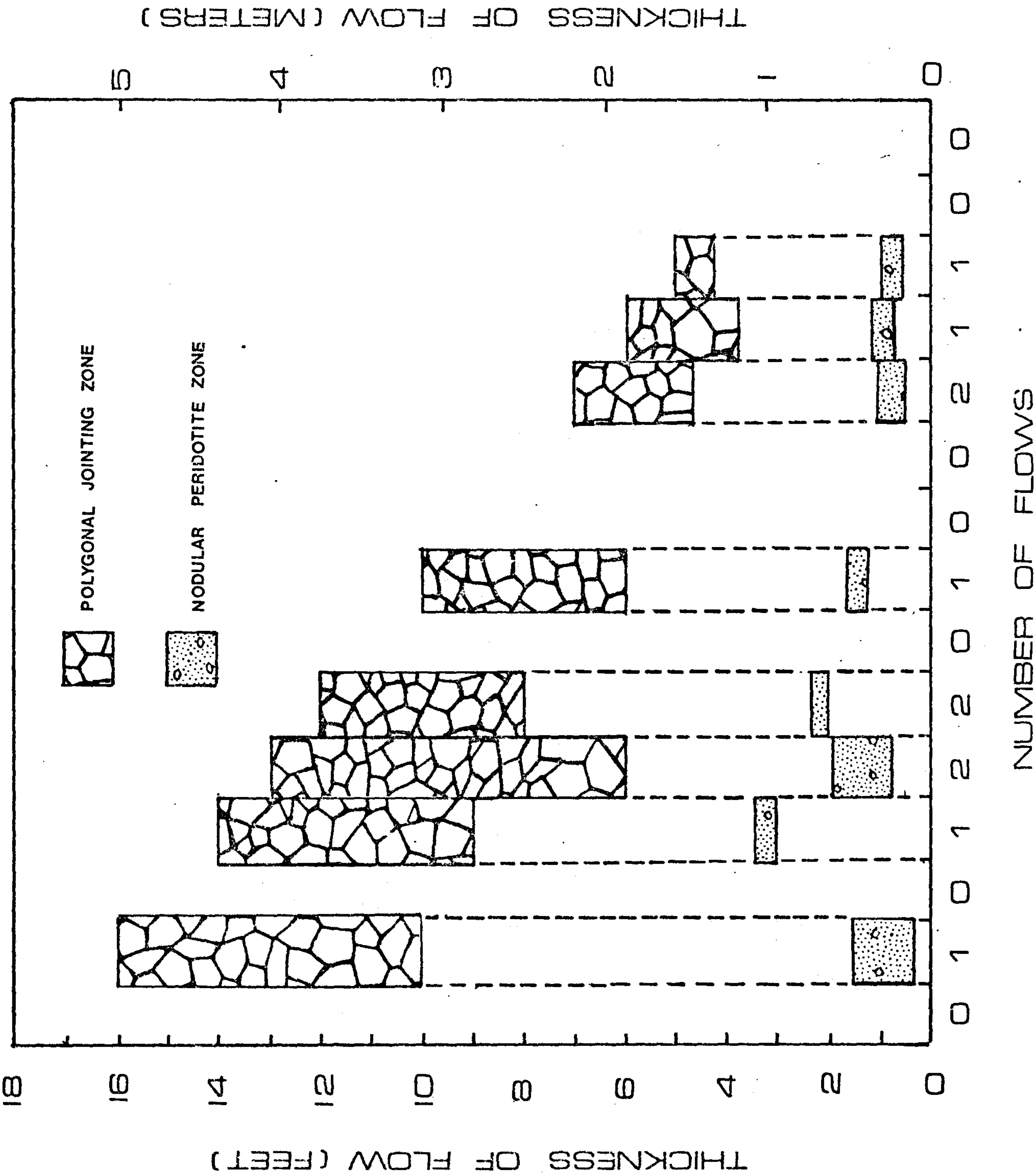
THICKNESS OF FLOW (METERS)
THICKNESS OF FLOW (FEET)
NUMBER OF FLOWS
POLYGONAL JOINTING ZONE
NODULAR PERIDOTITE ZONE

CHAPTER 3

Petrography of Knobby Peridotites

3.1 Modal Analysis of Knobby Peridotites

Due to the difficulty in distinguishing the high proportion of devitrified glass from olivine and pyroxene phenocrysts, point counting of thin sections was required. Individual mineral proportions were calculated from 1000 point counts and converted to the percentage figures shown in Appendix 1.

3.2 Mineralogy

In most thin sections, olivine occurs in clusters of rounded equant grains. The optical properties of these equant grains are consistent with forsterite (Kerr, 1977). Interstitial to these clusters is a crystalline matrix of devitrified glass and skeletal clinopyroxene (plate 4,5).

Olivine phenocrysts are usually equant in shape averaging from 0.5 millimeters to 0.7 millimeters; however, a few elongate grains averaging about 1.2 millimeters in length and 0.5 millimeters in width do occur. Most olivine crystals have been fractured and replaced by magnetite and serpentine (plate 5, 6, 7). Serpentine initially invades the olivine crystal within fractures and along grain boundaries. Advanced alteration of olivine to serpentine produces pseudomorphs that retain the original olivine form (plate 4). More extreme alteration may produce pseudomorphs of lizardite which exhibit a characteristic hour glass texture. (plate 8)

In the early stages of serpentinization, magnetite forms fine, discrete dust that concentrates along the rims of the serpentine and within olivine fractures. With more advanced alteration, portions of the magnetite will collect into fine bands that crosscut the serpentine. In some pseudomorphs after olivine, magnetite dust is heavily disseminated throughout.

Euhedral chromite is found within and adjacent to weakly altered olivine (plate 7), however, most chromite is subhedral and surrounded by a rim of magnetite. The subhedral chromite is usually located within the interstitial glass.

The interstitial glass is usually clear, but may produce by devitrification a finely crystalline reddish-brown matrix. Devitrification of the interstitial glass produces clinopyroxene (compatible with optical properties of diopsidic augite (Kerr, 1977)), orthopyroxene, olivine and traces of plagioclase. Elongate skeletal grains of augite form into parallel growths that crosscut the matrix (plate 5) or form acicular growths that radiate from the grain margins of relict olivines (plate 7). Larger dendritic augite (average 0.4 millimeters in length) and skeletal olivine (plate 6) form but are less common.

Some clinopyroxene (Figure 9) and most of the orthopyroxenes have been completely replaced during serpentine alteration to form bastite pseudomorphs. Due to this alteration, most orthopyroxene identification is based on texture and crystal form. Only a few ragged relict grains of plagioclase remain, but these are extensively sauseritized.

Tremolite replaces serpentine and augite producing poikioblastic laths that crosscut olivine grains along planes of weakness (plate 10). Tremolite laths also form in random clusters within the glass matrix. Particles of magnetite can be found within tremolite grains.

3.3 Interpretation

Olivine and chromite are the two main cumulus minerals. The proportion of olivine is dependent on the degree of metamorphic alteration. Slightly altered flows contain 38 - 45 per cent olivine, while severely altered flows may carry only two per cent relict olivine. Since euhedral chromite is found within olivine crystals, chromite must have begun to crystallize before all the olivine had formed. Skeletal growths of clinopyroxene, orthopyroxene, olivine and plagioclase within the glass matrix indicates rapid cooling during devitrification.

The introduction of H_2O converts ultramafic rocks into serpentinites. The presence of serpentine in a rock indicates that the fluid phase present during rock alteration contained very little CO_2 or none at all (Winkler, 1980). Tremolite is considered a metamorphic mineral because it replaces clinopyroxene in the matrix and serpentine in the olivine clusters. Tremolite, according to Winkler (1980), stabilizes at higher temperatures than diopsidic augite and persists over a large temperature range.

3.4 Comparison of Other Cumulus Zone

The petrography of the knobby peridotite deviates only slightly from that of the remaining portion of the cumulus peridotite. Pyke *et al*

(1973) observed that the cumulus peridotite contained 65 per cent olivine and less than ten per cent glass. The knobby peridotite contains less than 45 per cent olivine and has a correspondingly higher proportion of interstitial glass and serpentine. Pyke _et al_ (1973) observed only 15 per cent alteration of olivine, while knobby peridotite zones experienced more extensive alteration.

The accessory minerals clinopyroxene, orthopyroxene, and tremolite are present in comparable proportions in both peridotite and knobby peridotite zones.

3.5 Knobby Peridotites

The development of knobby protuberances imply a change in mineralogy within the knobby peridotite band.

Observations of cut slabs (plate 12) indicate that knobs within the peridotite are intimately associated with dark veins that cut through the slab. These veins when observed in thin section are composed of devitrified glass. Thin sections cut parallel to the weathered surface again show direct correlation between knobby protuberances and a concentration of glass matrix. Circular concentrations of glass in the thin sections are often connected to one another by narrow glassy veins. This is consistent with observations on the weathered surface that reveal narrow protruding ridges between the individual knobs.

In some circular glass accumulations, skeletal needles of clinopyroxene concentrate in random clusters (plate 11). These laths are strongly zoned and often bend conforming to the boundaries of the matrix. Nesbitt (1971) describes such textures in pyroxenitic komatiites as pyroxene spinifex, which implies rapid cooling. Hatch (1926) describes this type of concentric growth as a perlitic texture. The curving of the clinopyroxene is due to cooling where the internal portion is still undergoing contraction. The circular shape of the knobby peridotite may be a result of the rapid cooling of the interstitial glass.

PLATE 4

Equant, cumulus olivine (01) within an interstitial devitrified glass matrix. Pseudomorphs of olivine (Serp) are cut by tremolite fibers (Tr).

Sample PH-3 (63X).

PLATE 5

Parallel skeletal grains of clinopyroxene (Cpx) form a network within the glass matrix. Olivine grains (01) show alteration to serpentine (Serp.)

Sample PH-6 (160x).

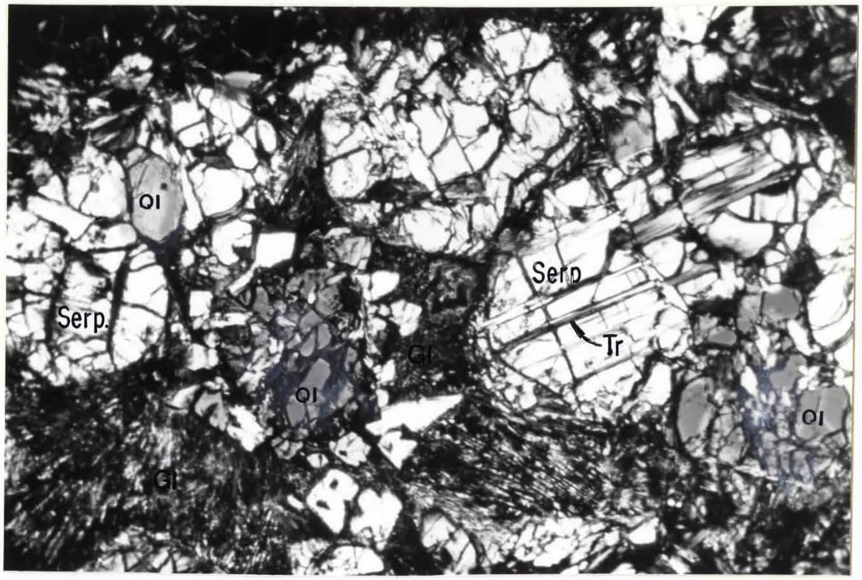
Ol
Serp.
Serp
Tr
Gl
Ol
Ol
Gl

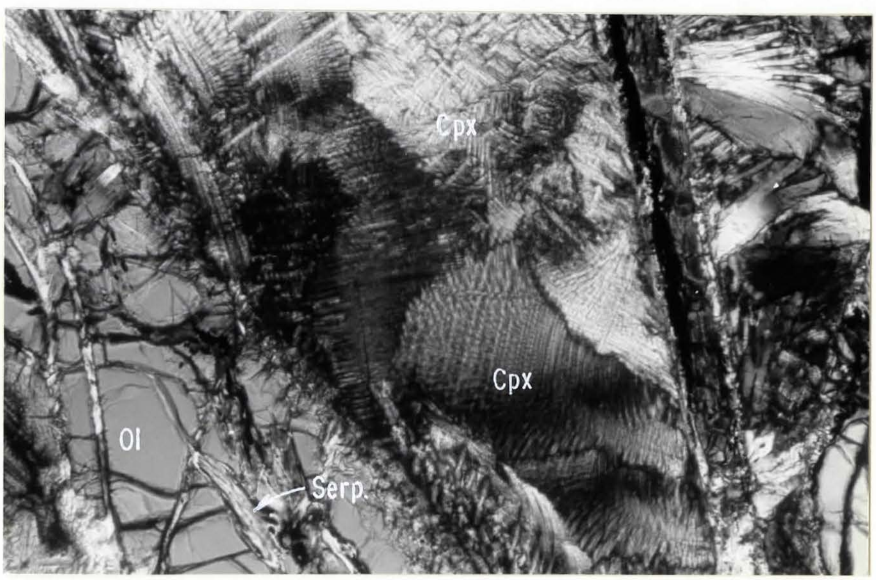
Cpx
Cpx
Ol
Serp.

PLATE 6

Mildly serpentinized cumulus olivine (01) lies adjacent to a devitrified glass matrix (Gl) containing skeletal olivine (01_2) and augite (Cpx).

Sample PH-6 (160x).

PLATE 7

Serpentine (Serp) and magnetite (Mag) alteration along fractures in the cumulus olivine. A circular augite (Cpx) radiates from the olivine grain margins. Note chromite spinel (Chr) adjacent to the olivine.

Sample PH-9 (160x).


Cpx
Gl
Ol2
Ol2
Ol1

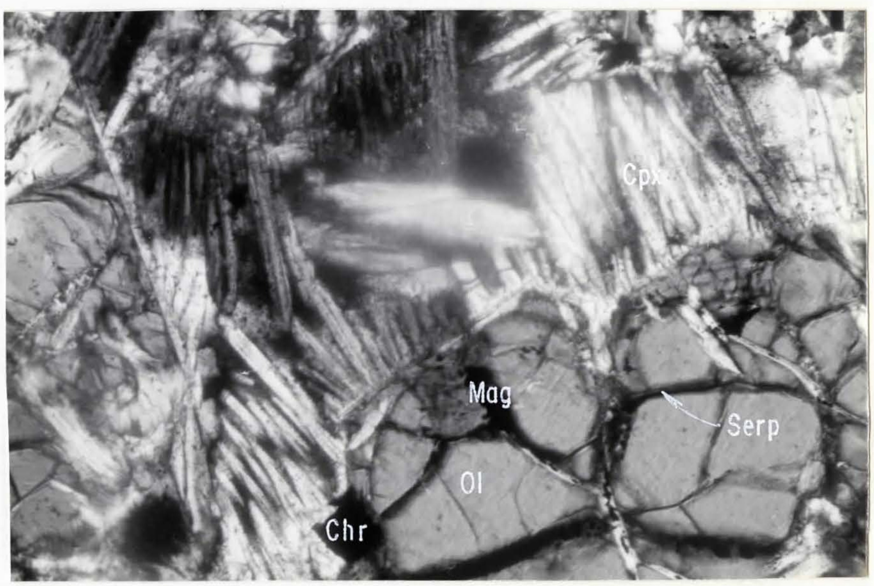
Cpx
Mag
Serp
Ol
Chr

PLATE 8

Serpentinized olivine exhibiting typical hour glass mesh texture. Serpentine is rimmed by magnetite.

Sample PH-2 (63x).

PLATE 9

Serpentinized laths of clinopyroxene (Cpx) within the devitrified glass matrix (Gl).

Sample PH-4 (63x).

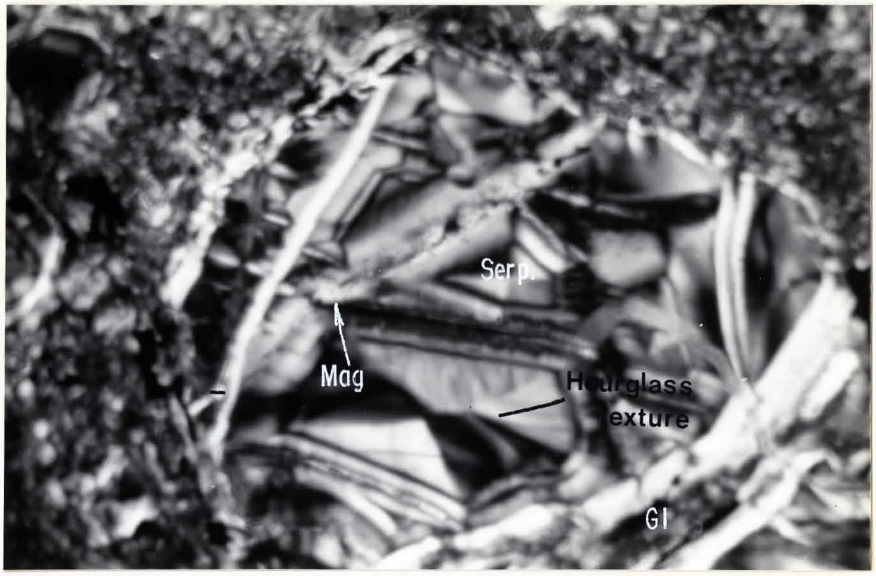
Serp.
Mag
Hourglass texture
Gl

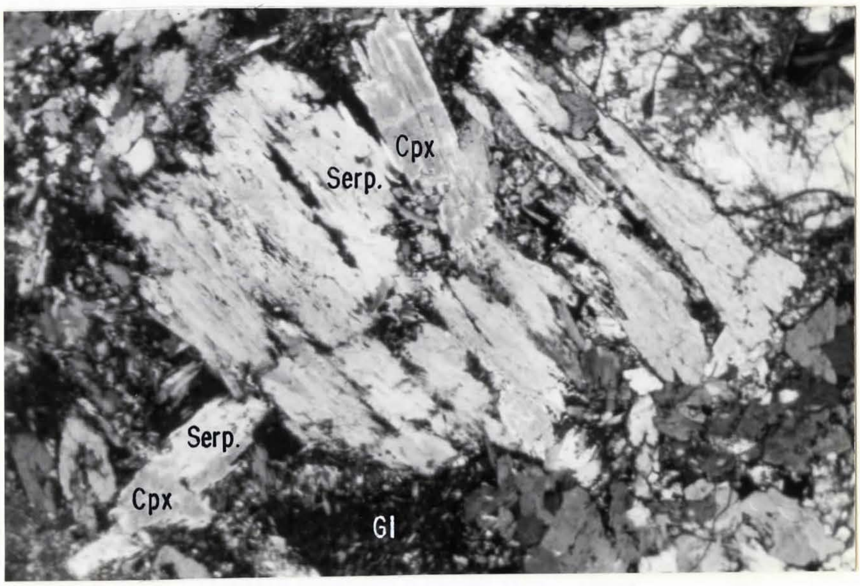
Cpx
Serp.
Serp.
Cpx
Gl

PLATE 10

Metamorphic tremolite (Tr) cuts olivine grains (Ol) along zones of weakness.

Sample PH-7 (160x).

PLATE 11

Devitrified clinopyroxene (Cpx) within the glass matrix (Gl). Note random orientations of clinopyroxene. Typical texture found within individual knobby peridotites.

Sample PH-5 (63x).

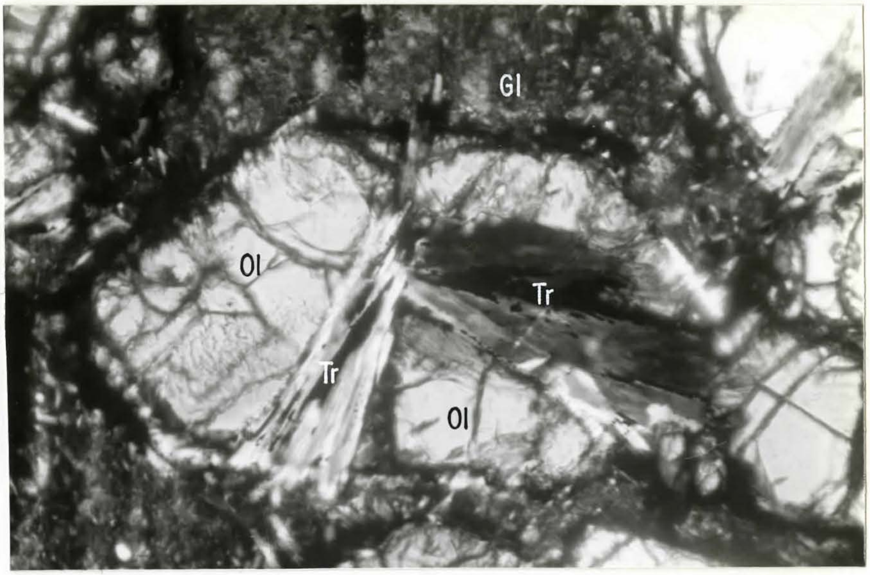
Gl
Ol
Tr
Tr
Ol

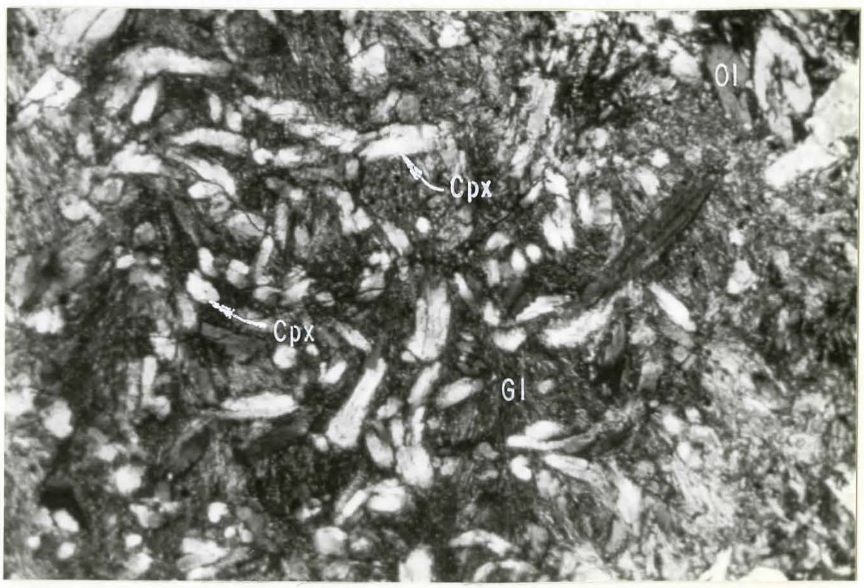
Ol
Cpx
Cpx
Gl

PLATE 12

Cut slab of knobby peridotite. Interstitial glass (outlined in black) contains more resistent material producing knobby proturberances on erosion surfaces (A_1).


A1

CHAPTER 4

Opaque Mineralogy

Optical properties, microhardness and microchemical tests were used to identify opaque reflecting minerals. Observations from three polished sections (PH-2, PH-10, PH-16) and six polished thin sections (PH-3, PH-6, PH-10, PH-16, PH-17-1, PH-17-2) were used to define representative assemblages. The opaques identified were chromite, magnetite and heazlewoodite.

4.1 Chromite

Chromite was recognized by its dark grey colour and isotrophism under reflected light. Microhardness measurements give a range of 1006 - 1027 VH with an average of 1022 VH for six measurements. These microhardness tests compare with a chromite VH range of 1036-2000 in Uytenbogaard and Burke (1971) and a mean of 1305 VH (McLeod and Chamberlain, 1969).

Chromite is common in every slide, but never exceeds one per cent by volume. Isolated euhedral chromite grains are present but subhedral chromite rimmed and included by magnetite (plate 15) forms the predominant chromite morphology and mineral association. Euhedral chromites usually appear within or adjacent to mildly altered olivines, while subhedral chromite is located in the serpentinized zone surrounding the relict olivine in more altered ultramafics.

TABLE 1

OPTICAL PROPERTIES AND MICROHARDNESS TESTS

Mineral	Colour	Anisotrophism	Microhardness		Microhardness	
			Readings (Average)	Range	[Uyten. & Burke] Range	[McL. & Chamb.] Mean
Chromite	Dark grey - Brownish Grey	Isotropic	1017 1006 <1027 <1027 <1027 <1027 (<1022)*	1006- 1027	1036-2000	1305
Magnetite	Grey, with Brownish Tint	Isotropic	458 488 514 525 529 508 471 (499)	458-529	440-110	581
Probable Sulfide	Creamy Yellow	Distinct - Greenish grey to greyish blue	293 268 283 274 283 274 (279)	268-293		

* ( ) measured average.

TABLE 1

OPTICAL PROPERTIES AND MICROHARDNESS TESTS

Mineral	Colour	Anisotrophism	Microhardness		Microhardness	
			Readings (Average)	Range	[Uyten. & Burke] Range	[McL. & Chamb.] Mean
Chromite	Dark grey - Brownish Grey	Isotropic	1017 1006 <1027 <1027 <1027 <1027 (<1022)*	1006- 1027	1036-2000	1305
Magnetite	Grey, with Brownish Tint	Isotropic	458 488 514 525 529 508 471 (499)	458-529	440-110	581
Probable Sulfide	Creamy Yellow	Distinct - Greenish grey to greyish blue	293 268 283 274 283 274 (279)	268-293		

* ( ) measured average.

TABLE 2

COMPARISON OF SULFIDE MINERALS

Mineral	Colour	Anisotrophism	Measured	Microhardness	
				[Uyten. & Burke] Range	[McL. & Chamb.] Mean
Probable Sulfide	Creamy Yellow	Distinct - Greenish grey to greyish blue	268-293 (279)	-	-
Heazelwoodite	Creamy Yellow	Strong - Greenish grey to greyish blue	-	221-274	275
Pyrrhotite	Cream with faint pinkish brown	Strong - Yellowish grey, greenish grey or greyish blue	-	230-390	278

TABLE 3

MICROCHEMICAL TESTS

Chemical	Observed Results	Heazelwoodite (Chamberlain)	Pyrrhotite (Short)
$FeCl_3$	Negative	Irridescent	Negative
HNO_3	Stains Yellowish Brown (Gold Colour)	Greyish Brown	Stains Light Brown
HCl	Faint Brown to Negative	Faint Brown	Drop Turns Yellow But Surface Does Not Stain
$HgCl_3$	Distinct Brown	Stains Brown	Negative

Chromite is the dominant relict cumulus mineral observed in reflected light and often serves as a nucleus for secondary magnetite accumulations. Magnetite embayments in the chromite indicate that chromite also alters to magnetite.

4.2 Magnetite

Magnetite was identified on the basis of its light grey colour and its isotrophism under reflected light. Microhardness tests indicate a range between 458 - 529 VH with an average of 499 VH for seven measurements. Uytenbogaard and Burke (1971) give a magnetite hardness range of 440 - 1100 VH and a mean of 581 VH (McLeod and Chamberlain, 1969).

Magnetite is common in every slide and ranges in modal percentage from one to five per cent. Granular aggregates of magnetite are found in isolated clusters (0.01 mm to 0.1 mm in width) or as dendrites between skeletal clinopyroxene (plate 16). Magnetite rims and includes chromite (see section 4.1) and forms intimate intergrowths with the sulfide minerology (see section 4.3). Magnetite usually occurs with serpentine, either within olivine fractures (plate 18) or in alteration zones surrounding relict olivine.

Magnetite is a product of serpentinization (see section 3.3) thus it constitutes a secondary mineral assemblage.

4.3 Sulfides

Sulfides are much less widespread than oxides with only trace amounts identified in the polished section PH-10. Reflected light observations indicate a creamy yellow mineral that exhibits a distinct anisotrophism of greenish grey to greyish blue. Microhardness analysis produced a range of 268 - 293 VH with an average of 283 VH for six measurements. Potential sulfide mineral properties (for Heazlewoodite and Pyrrhotite) are shown in Table 2.

a) Microchemical Tests

Microchemical tests were carried out and compared with liturature results for heazlewoodite and pyrrhotite (Table 3). Due to the arbitrary nature of colour identification the results of the tests were inconclusive. A microchemical test for nickel was undertaken since the heazlewoodite (Ni, Fe) S should produce a more distinct reaction than pyrrhotite (FeS).

The process used involved:

1) HNO_3 solution to clean the sample.

2) Application of dimethyl glyoxide to the sulfide.

Only two out of the eight sulfides tested reacted to produce the pinkish colour diagnostic of a nickel reaction. The lack of conclusive results may reflect the weakness of the test rather than the lack of nickel in the sulfides.

b) X-Ray Diffraction

An attempt to use X-ray diffraction was unsuccessful due to the lack of recoverable sulfide grains.

c) Scanning Electron Microscope

At this point sulfide mineral identification is confined to a choice between heazlewoodite or pyrrhotite. A scanning electron microscope will be used to define the chemical constituents within the sulfide.

Samples of polished sections were scanned by X-ray emissions using an SEM Stereoscan. Detector windows in the SEM were set to record distributions of S, Fe and Ni.

i) Scan #1

The optical subject (plate 13-A) indicates that two distinct minerals are present within the grain. The sulfur scan (plate 13-B) shows that the lighter mineral contains significant amounts of sulfur, while the dark mineral contains minor sulfur. Nickel (plate 13-C) is confined to the sulfide, while iron content (plate 13-D) is high in both minerals with higher concentrations in the dark mineral.

The nickel sulfide mineral (light mineral-plate 13-A) is probably heazelwoodite. Heazelwoodite is compatible with the inferred SEM composition and the microhardness, anisotropism and colour of the probable sulfide (Table 1). Pyrrhotite is less compatible because it has a weaker anisotropism and a low nickel content. Other nickel sulfides are ruled out for a number of reasons. Pentlandite $(Fe, Ni)_9S_8$, Violarite $(Ni, Fe)_3S_4$, and Awariute $(Ni, Fe)_3S_4$ are isotropic (Uytenbogaart and Burke, 1968) while Millerite formation is confined to talc carbonate environments (Eckstrand, 1975).

ii) Scan #2

The optical subject (plate 14-A) indicates a cluster of monomineralic grains. Sulfur distribution (plate 14-B) outlines the observed crystal form while the nickel scan (plate 14-C) shows a coincidence of nickel and sulfur rich regions in the slide. The iron scan (plate 14-D) shows dispersion which probably reflects a background reading. No concentration of iron was evident in the crystal areas.

PLATE 13 SCANNING ELECTRON MICROSCOPE

Referred to as Scan #1 in text.

A - dark mineral is magnetite (Mgt)
light mineral is heazelwoodite (Hz)

B - sulfur scan

C - nickel scan

D - iron scan

A

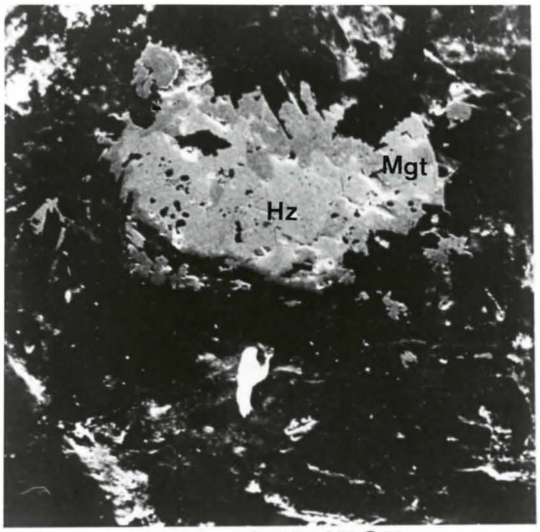

OPTICAL SUBJECT

D

IRON DISTRIBUTION

SULFUR DISTRIBUTION

B

NICKEL DISTRIBUTION

C

PLATE 14 SCANNING ELECTRON MICROSCOPE

Referred to as Scan #2 in text.

A - mineral grains - heazelwoodite (Hz)

B - sulfur scan

C - nickel scan

D - iron scan

A

OPTICAL SUBJECT

D

IRON DISTRIBUTION

SULFUR DISTRIBUTION

B

NICKEL DISTRIBUTION

C

The results of the scan indicates a nickel sulfide compatible with the optical and microhardness properties of heazelwoodite.

A number of sulfide grains were scanned giving results indicative of a nickel sulfide, specifically heazelwoodite.

4.4 Nickeliferous Mineral Assemblages

Serpentinization of ultramafic rocks generates H_2 (Winkler, 1980) creating a reducing environment best suited for low sulfur minerals. Nickel (1959) believes that nickel in serpentinites was derived from iron and nickel originally present in primary relict structures. Chamberlain (1960) suggests that olivines have sufficient magnesium to combine with other silicates present to form serpentine with excess nickel and iron producing magnetite and nickel rich sulfides.

Using the Dumont ultramafic body in northern Quebec, Eckstrand (1975) has determined the stability fields of nickeliferous sulfides and silicates as a function of pS_2 and pO_2. These results are in turn related to the degree of alteration in silicate rocks. At low temperatures, the stable assemblage in close proximity to relict olivine grains is:

pyrrhotite + pentlandite + magnetite

The redistribution and accumulation of oxygen (increasing fO_2) and sulfur (increasing fS_2) coincide with advanced serpentinization and result in the following series of stable mineral assemblages:

1. magnetite + awaruite + heazelwoodite
2. magnetite + heazelwoodite

Eckstrand (1975) believes that the nickel originally contained in silicate form (eg. olivine) is in part converted during serpentinization to opaque mineralogy. When sulfur is present, the opaque minerals resulting from alteration of olivine are dependent on the amount of sulfur present and the fO_2 environment produced by alteration. The formation of a heazelwoodite magnetite assemblage is restricted to the specific sulfur and oxygen fugacities defined in Figure 11.

An alternative explanation suggests that the original magmatic sulfides are transformed by destruction and replacement to magnetite and Ni - Fe sulfides. The original sulfides, pyrrhotite and pentlandite, may have been replaced by awariute then heazelwoodite or could have directly altered to heazelwoodite. This second alternative is speculative because optical evidence is inconclusive.

FIGURE 11

fO_2 vs fS_2 diagram summarizing the ranges of fO_2 and fS_2 of opaque mineral assemblages in the three principle alteration facies of ultramafic rocks. Vertical line pattern indicated position of Pyke's Hill mineral assemblage relative to the alteration faces.

Fe	-	Iron	hz	-	Heazelwoodite
Mg	-	Magnesium	py	-	Pyrite
po	-	Pyrrhotite	ml	-	Millerite
aw	-	Awaruite	vi	-	Violarite
pn	-	Pentlandite	hm	-	Hematite

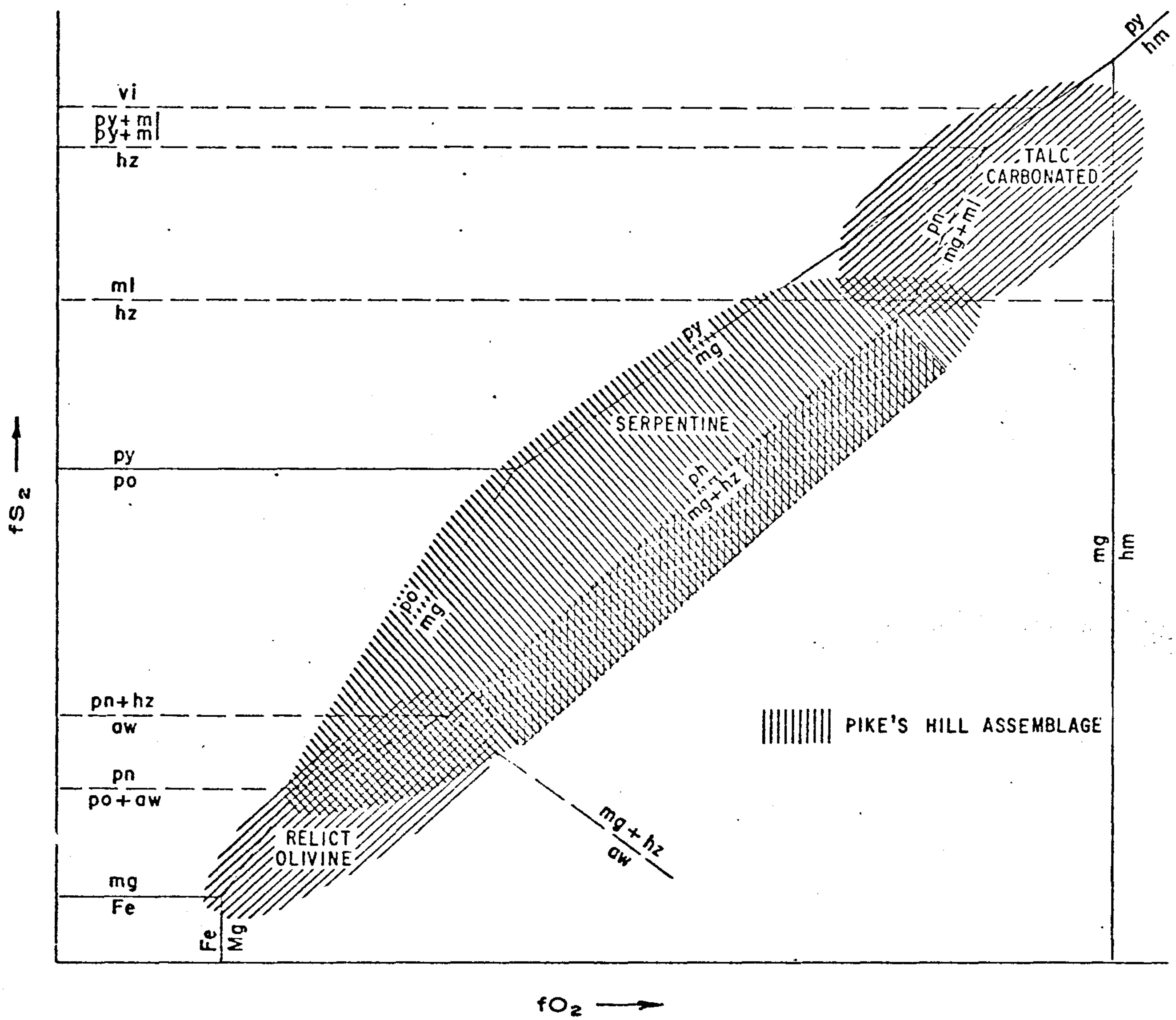
vi
py+ml
py+ml
hz
ml
hz
py
po
pn+hz
aw
pn
po+aw
mg
Fe
Fe
Mg
fS2
fO2
py
hm
TALC
CARBONATED
pn
mg+ml
py
mg
SERPENTINE
pn
mg+hz
po
mg
RELICT
OLIVINE
mg+hz
aw
mg
hm
PIKE'S HILL ASSEMBLAGE

PLATE 15

Chromite nucleus (Chr) surrounded and replaced by magnetite (Mag). Located in serpentine adjacent to relict olivine.

Sample PH-10.

light grey gangue - cpx
dark grey gangue - serp.

PLATE 16

Dendritic magnetite (Mag) forms between parallel skeletal clinopyroxene.

Sample PH-14

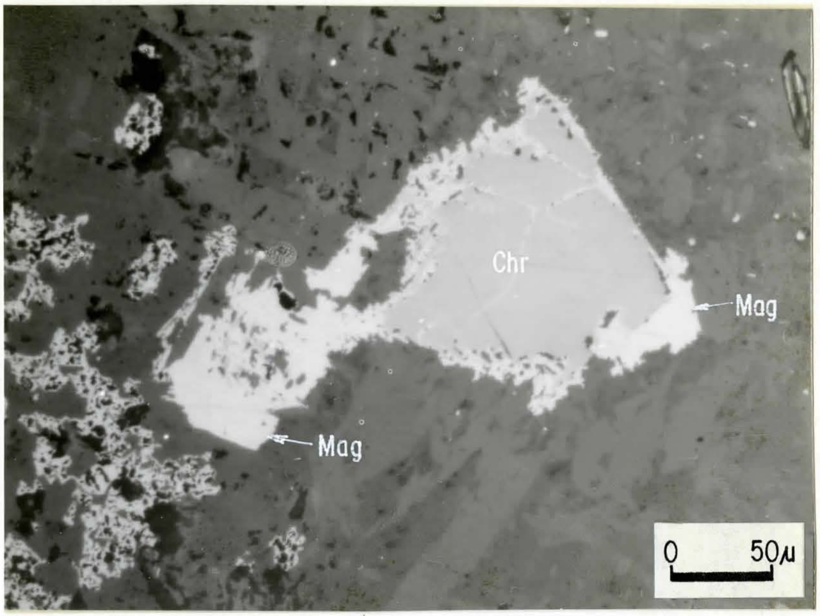
Chr
Mag
Mag
0 50µ

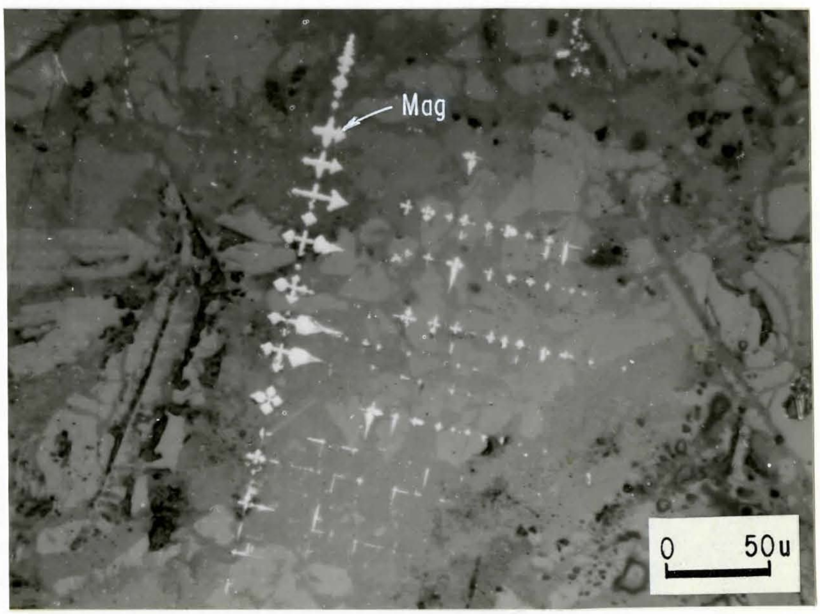
Mag
0 50u

PLATE 17

Intimate growth of heazlewoodite (Hz) with magnetite (Mag). Located in interstial glass matrix outside the fringes of the serpentinized olivine.

Sample PH-10.

PLATE 18

Magnetite (Mag) rims the olivine grain (01) and includes the olivine along fractures.

Sample PH-16.

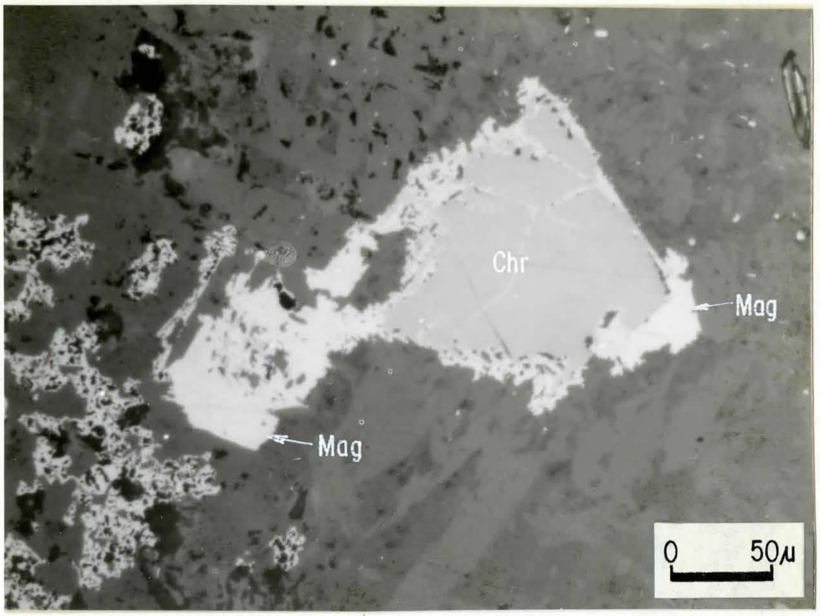
Chr
Mag
Mag
0 50μ

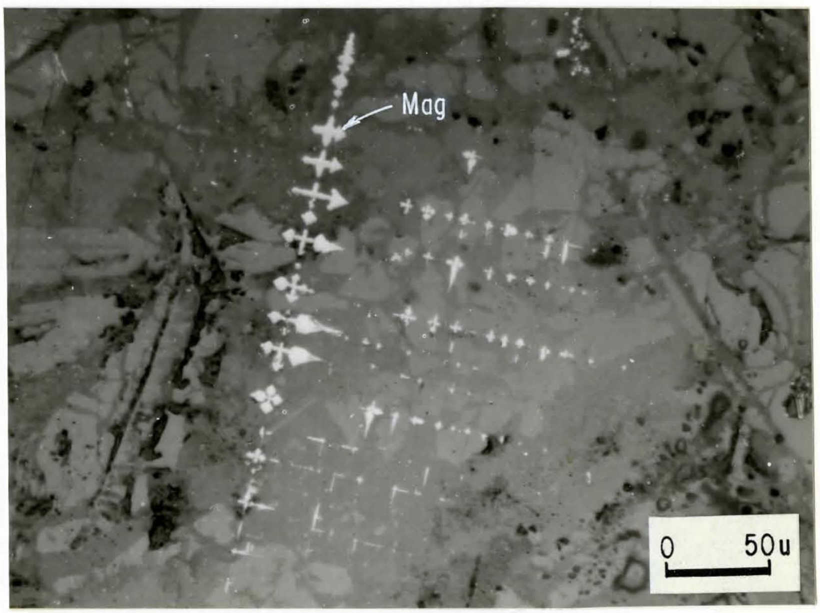
Mag
0 50u

CHAPTER 5

Geochemistry

5.1 Sample Preparation

A representative portion of each sample was crushed in a jaw crusher, ground in a disc pulverizer and then powdered in a tungsten carbide shatterbox to -200 mesh.

5.2 X-Ray Fluorescence

a) Major Elements

Fusion pellets, prepared using the procedure outlined by Hutchinson (1974) were analyzed on a Philips, Model 1450 AHP automatic, sequential X-ray fluorescence spectrometer. A Cr X-ray tube was used to analyze the major elements Si, Al, total Fe, Mg, Ca, Na, K, Ti, Mn, and P. Rock standards (GSP-1, NIM-D, NIM-G, NIM-N, W-1, BCR-1, JR-1, JG-1, SY-1, SY-2, SY-3) were used for calibration while one standard within the spectrometer acted as a drift monitor during analysis.

b) Trace Elements

Power pellets prepared using the method described by Marchand (1973) were analyzed with a Mo X-ray tube for Cr, Co, Pb, Cu, Zn, As, V, Ni, S.

5.3 LECO Analysis

The Leco gas analyzer at McMaster University was used to analyze both CO_2 and S. Leco analysis for sulfur was done by Otto Mudrock.

5.4 Neutron Activation

Analysis for gold was carried out by carrier based radiochemical neutron activation. Two runs containing 8 powder samples and three standards were irradiated for 12 megawatt hours in the McMaster Nuclear Reactor. After a cooling period of three days the samples were transported to the lab.

In the laboratory gold carriers were added to sample powders. The procedure used was adopted with minor modifications from Crocket et al (1968).

5.5 Data

The major elements and trace element data determined by XRF are in Table 4 and 5 respectively. The major elements are in weight per cent and the trace elements in ppm. The gold analysis are in Table 6 and expressed in ppb.

A comparison of mean and standard deviation for major elements and trace elements within different zones of the ultramafic komatiitic flow are presented in Table 7 and 8 respectively. Data for the spinifex and cumulus peridotites were collected from data produced in Arndt et al (1977), Pyke et al (1973) and MacRae (1981).

C.I.P.W. norms calculated using a computer program devised by Mattison (1973) are presented in Appendix 2.

5.6 Jenson Cation Plot

To further enhance the field characteristics, XRF datum are converted to cation norms and plotted on the Jenson Cation Plot (Jenson, 1976).

FIGURE 12

Jenson cation plot. Knobby peridotite samples are confined to ultramafic komatiitic field.

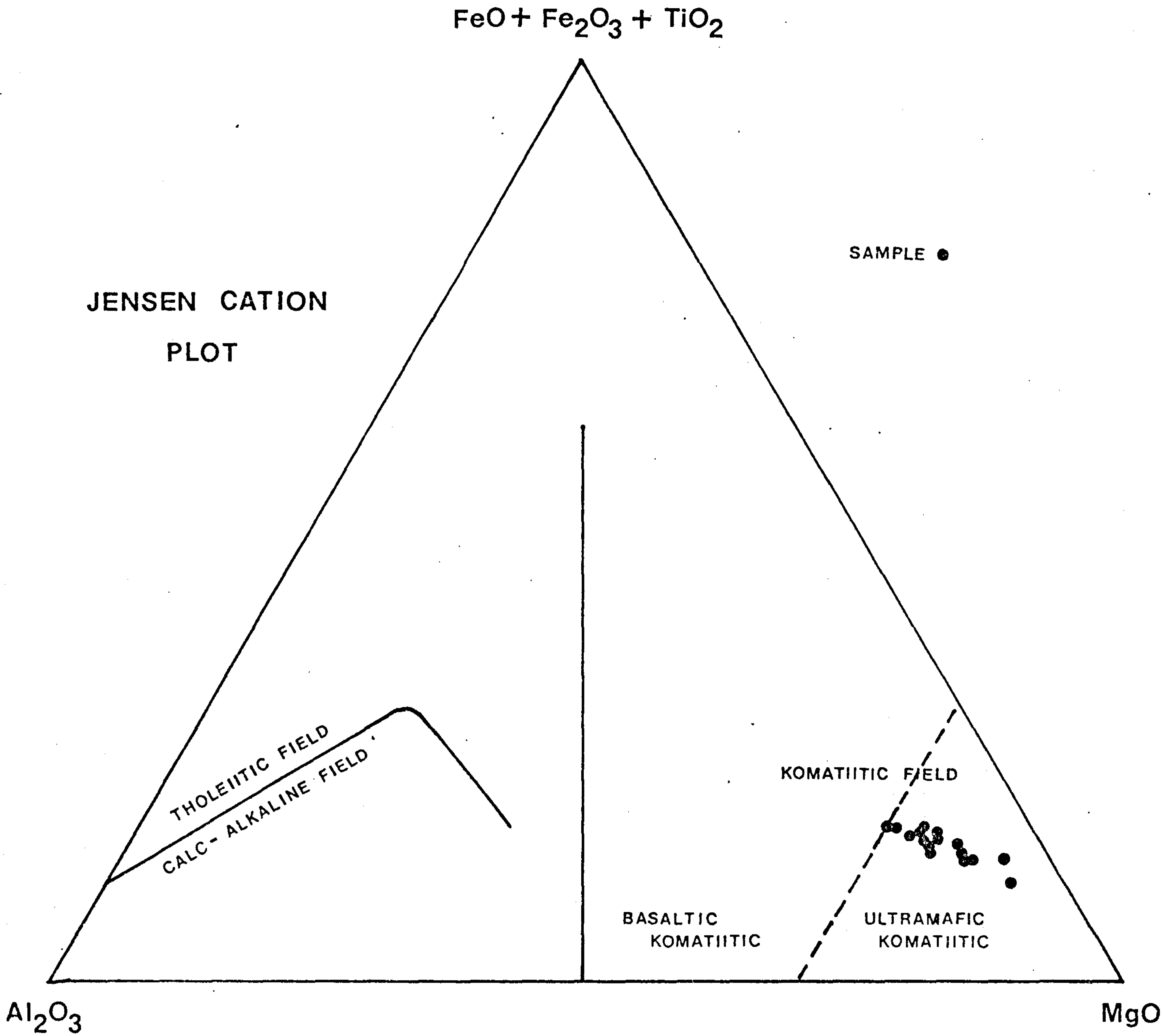
FeO + Fe2O3 + TiO2
JENSEN CATION PLOT
SAMPLE
THOLEIITIC FIELD
CALC - ALKALINE FIELD
KOMATIITIC FIELD
BASALTIC KOMATIITIC
ULTRAMAFIC KOMATIITIC
Al2O3
MgO

TABLE 4

MAJOR ELEMENT ANALYSIS

(Weight Percent Normalized to 100%)

Sample No.	SiO_2	Al_2O_3	Fe_2O_3	MgO	CaO	Na_2O	K_2O	TiO_2	MnO	P_2O_5	LOI	CO_2
PH1	37.36	2.72	11.21	37.90	1.26	0.44	0.01	0.14	0.17	0.02	8.79	0.314
PH2	39.07	2.96	9.78	39.38	0.37	0.37	0.01	0.18	0.20	0.01	7.67	0.238
PH3	40.79	4.40	11.36	35.03	4.25	0.37	0.06	0.24	0.19	0.00	3.23	0.311
PH4	42.47	6.34	12.34	27.64	6.58	0.57	0.10	0.34	0.21	0.00	3.40	0.425
PH5	40.25	4.47	11.68	34.59	4.28	0.64	0.05	0.24	0.19	0.00	3.60	0.216
PH6	39.83	4.10	12.31	32.77	3.61	0.44	0.03	0.23	0.18	0.00	6.40	0.524
PH7	41.00	5.53	11.92	31.26	5.30	0.45	0.03	0.30	0.22	0.00	4.00	0.341
PH9	42.58	6.08	12.60	29.56	6.05	0.74	0.09	0.33	0.25	0.00	1.72	0.458
PH10	41.10	4.36	11.47	35.33	4.27	0.49	0.05	0.24	0.22	0.00	2.49	0.440
PH11	42.55	6.49	12.52	26.80	6.54	0.80	0.11	0.35	0.22	0.00	3.62	0.307
PH12	41.62	5.40	11.93	31.16	5.53	0.41	0.07	0.29	0.20	0.00	3.39	0.444
PH13	40.70	5.61	12.45	31.19	4.49	0.52	0.03	0.31	0.21	0.00	4.49	0.521
PH14	40.70	4.88	12.98	31.05	4.84	0.43	0.08	0.28	0.23	0.00	4.54	0.336
PH15	41.82	5.55	12.69	29.87	5.51	0.80	0.09	0.31	0.22	0.00	3.14	0.385
PH16	42.47	5.74	12.67	30.90	5.86	0.85	0.07	0.30	0.23	0.00	0.91	0.343
PH17	41.12	5.12	12.68	31.19	5.06	0.55	0.04	0.27	0.24	0.00	3.74	0.411

LOI - Loss of Ignition

TABLE 5

TRACE ELEMENT ANALYSIS (P.P.M.)

Sample No.	CR	CO	PB	CU	ZN	AS	V	NI	S(XRF)	S(LECO)
PH1	1720	89	7	11	43	0	44	2920	400	300
PH2	1900	92	1	11	40	0	59	2820	400	400
PH3	1940	91	14	13	49	0	71	2330	400	300
PH4	2280	80	13	22	63	0	105	1710	600	400
PH5	2020	91	14	23	51	0	77	2340	500	400
PH6	2160	104	11	10	43	0	76	2520	400	600
PH7	2180	90	14	25	52	0	97	1850	500	300
PH9	2250	78	13	14	56	0	109	1780	400	300
PH10	1930	88	14	23	49	0	75	2350	600	300
PH11	2370	86	10	45	67	0	108	1630	600	300
PH12	2100	84	9	13	51	0	87	1910	500	400
PH13	2460	86	11	10	46	0	116	1930	500	300
PH14	2100	101	8	13	59	0	88	2050	400	300
PH15	2220	91	10	92	72	0	94	1900	600	300
PH16	2340	88	12	33	58	0	95	1850	500	300
PH17	2210	97	13	21	56	3	94	2010	400	300

TABLE 6

GOLD CONTENT OF SAMPLES

Sample	Weight MGM	PPB (Gold Content)
PH-1	213.30	0.28
PH-2	189.56	2.65
PH-3	271.19	1.47
PH-4	219.89	2.27
PH-5	240.08	1.27
PH-6	209.77	3.04
PH-7	220.17	0.55
PH-9	232.81	1.94
PH-10	267.90	1.37
PH-11	202.52	1.39
PH-12	266.20	5.78
PH-13	238.84	1.85
PH-14	251.02	3.04
PH-15	237.39	1.78
PH-16	236.92	1.67
PH-17	219.33	1.46

TABLE 7

COMPARISON OF MEAN AND STANDARD DEVIATIONS FOR MAJOR ELEMENTS

	SiO_2	Al_2O_3	Fe_2O_3	MgO	CaO	Na_2O	K_2O	TiO_2	MnO	P_2O_5	LOI	CO_2
	KNOBBY PERIDOTITE (16) [1]											
Mean	40.96	4.98	12.04	32.20	4.61	0.55	0.06	0.27	0.21	0.001	5.87	0.33
S.D.	1.40	1.09	0.81	3.43	1.72	0.16	0.03	0.06	0.02	0.001	2.57	0.14
	PERIDOTITE (7) [2]											
Mean	40.80	5.48	9.03	31.10	4.31	0.24	0.12	0.22	0.14	0.04	5.70	03.7
S.D.	1.16	1.11	1.96	3.24	1.22	0.14	0.06	0.07	0.03	0.01	3.46	0.06
	SPINIFEX (8) [2]											
Mean	43.37	7.84	11.18	23.44	7.04	4.51	0.11	0.34	0.18	0.02	4.96	0.36
S.D.	1.74	1.35	0.95	2.62	0.98	3.26	0.06	0.08	0.04	0.003	2.36	0.04

S.D. - Standard Deviation

(n) - Number of Analysis Used in Calculation

LOI - Loss of Ignition

1 - Data from this work

2 - References for peridotite data from Arndt et al (1977), Pyke et al (1973), MacRae W., (1981)

TABLE 8

COMPARISON OF MEAN AND STANDARD DEVIATIONS FOR TRACE ELEMENTS

	Cr	Co	Pb	Cu	Zn	As	V	Ni	S (XRF)	S (LECO)
	KNOBBY PERIDOTITE (16) [1]									
Mean	2136.00	89.75	10.86	23.86	53.40	0.00	87.10	2117.90	481.20	325.00
S.D.	195.00	6.80	3.46	20.58	8.91	0.00	19.30	386.30	83.41	118.32
	PERIDOTITE (6) [2]									
Mean	2243.00	105.50	5.67	24.00	66.00	0.00	-	2021.80	315.60	-
S.D.	398.70	8.96	0.58	4.58	8.48	0.00	-	198.30	48.00	-
	SPINIFEX (7) [2]									
Mean	2402.00	101.00	7.33	26.00	78.50	-	-	1376.30	170.10	-
S.D.	473.00	0.78	1.15	16.43	12.80	-	-	354.70	143.50	-

S.D. - Standard Deviation

(n) - Number of Analysis Used in Calculation

1 - Data from this work

2 - References for peridotite data from Arndt et al (1977), Pyke et al (1973), MacRae, W., (1981)

FIGURE 13

Mean and standard deviation of oxides at different zones within the peridotite flow. Graphical representation of data shown in Table 7.

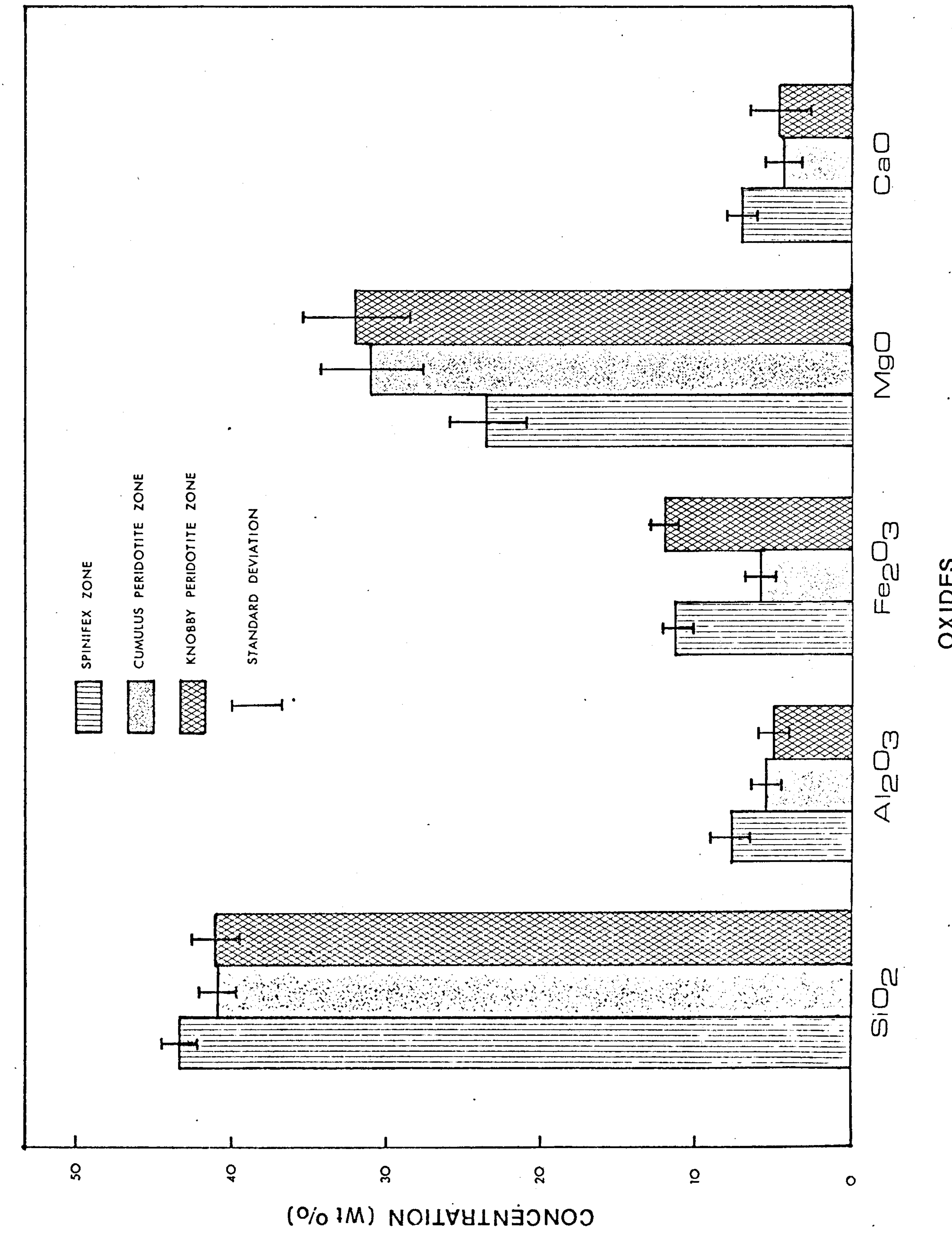
SPINIFEX ZONE
CUMULUS PERIDOTITE ZONE
KNOBBY PERIDOTITE ZONE
STANDARD DEVIATION
SiO2
Al2O3
Fe2O3
MgO
CaO
OXIDES
CONCENTRATION (Wt %)
0
10
20
30
40
50

Figure 13 is an enlarged protion of the Mg tholeiite field showing the groupings of the samples.

5.7 Major Elements

In comparing the geochemical character of the different zones within a peridotite lava flow, alteration effects and the mobility of elements during emplacement, burial and metamorphism must be considered. Naldrett (1964) found that during serpentinization alkali elements, Ca and to a lesser extent Si were quite mobile, while Mg, Fe, T, and Al were found to be relatively stable. Arndt et al (1977) considers movement of most major elements insignificant in all but the most highly altered rocks. Since only slight alteration has occurred in most samples, migration of elements will not be considered.

Assuming normal distribution, standard deviation is used to determine the significance of differences in average metal composition at different facies. With the exception of iron (FeO), major element figures show no major deviations in composition from the cumulus peridotite zone to the knobby peridotite zone.

The concentration of iron is greater in both the spinifex zone and the knobby peridotite zone than the cumulus zone. This difference in iron content may be attributed to analytical weaknesses in the data or to the higher concentrations of devitrified augite crystals and anomalous chlorite found in the glass matrix (Grubb, 1974).

Microprobe analysis of olivines in cumulus rock at Pyke's Hill (Arndt et al, 1977) determined forsterite (Mg_2SiO_4) content ranges from 85

FIGURE 14

Mean and standard deviation of trace elements of different zones within the periodite flow. Graphical representation of data shown in Table 8.

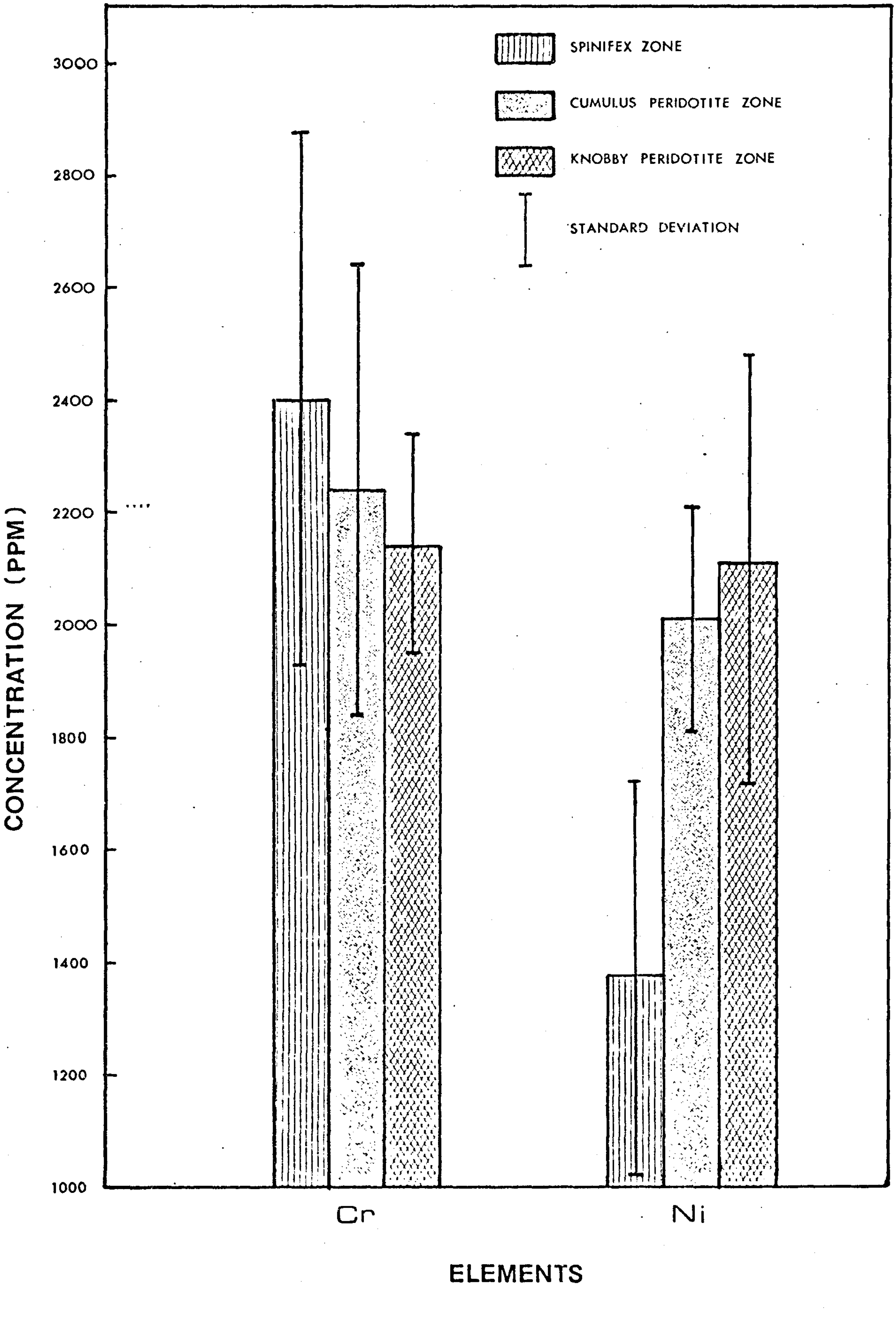
SPINIFEX ZONE
CUMULUS PERIDOTITE ZONE
KNOBBY PERIDOTITE ZONE
STANDARD DEVIATION
3000
2800
2600
2400
2200
2000
1800
1600
1400
1200
1000
CONCENTRATION (PPM)
Cr
Ni
ELEMENTS

FIGURE 15

Mean and standard deviation of cobalt of different zones within the peridotite flow. Graphical representation of data shown in Table 8.

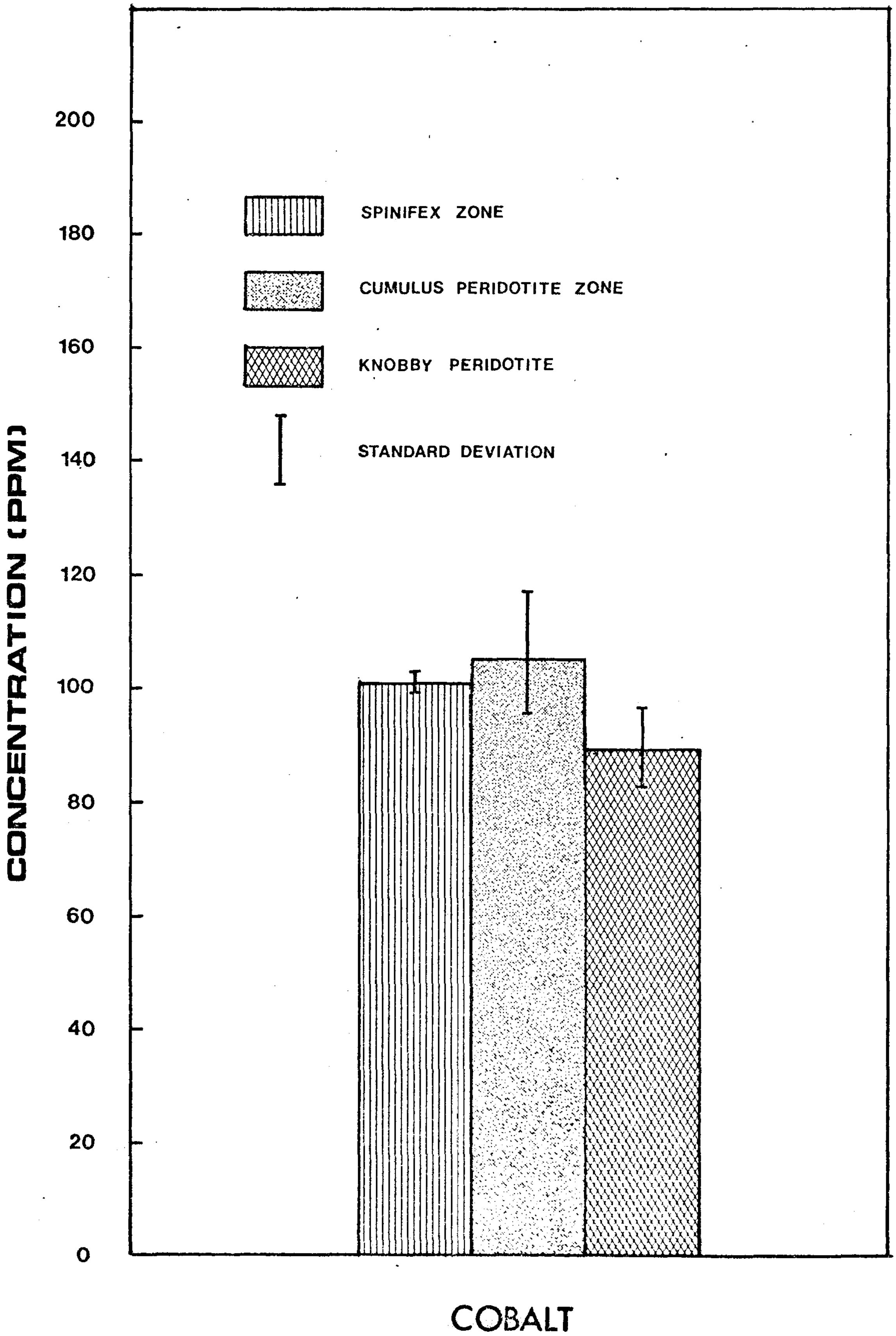
CONCENTRATION (PPM)
200
180
160
140
120
100
80
60
40
20
0
SPINIFEX ZONE
CUMULUS PERIDOTITE ZONE
KNOBBY PERIDOTITE
STANDARD DEVIATION
COBALT

to 90 mole per cent. The depleation of olivine in the spinifex zone due to fractional crystallization and settling leaves a residual containing a greater proportion of iron. Knobby peridotite zones contain fewer olivine crystals than overlying cumulus zones, thus the Fe^{2+}/Mg^{2+} ratio is greater in the knobby peridotite zone.

The spinifex zone has greater concentrations of SiO_2 and CaO with lower concentrations of MgO relative to the cumulus zones. Due to the high Mg content of olivines, greater accumulations of olivine in the cumulus zones result in higher MgO values.

Since the mole fractions of SiO_2 and CaO in olivines are less than in pyroxenes, olivine depleation in the spinifex zone increases the proportion of pyroxenes. The increased pyroxene proportion in the spinifex zone relative to the cumulus zones result in greater SiO_2 and CaO concentrations. SiO_2 and CaO may also show higher concentrations in the spinifex zone due to contamination in the upper levels of the flow by seawater.

5.8 Trace Elements

Chromium values in the cumulus zone are slightly lower than the spinifex zone since chrome spinel forms after most of the phenocryst olivine has crystallized and settled to the base of the flow (Arndt, 1975). According to Gunn (1971), olivines are usually poor in chromium while the environment the olivine crystallize in are rich in chromium due to spinel inclusions.

Nickel and chromium values usually display a covariance due to the association of nickel with mafic silicates and spinels (Turekian, 1978).

This correlation is not evident in the analysis of Pyke's Hill ultramafics. The spinifex zone has the highest concentration of chromium, but has the lowest nickel concentration of the three zones. Olivine is a major sink for nickel thus the cumulus facies whould accommodate significantly more nickel, regardless of the chromium composition.

Cobalt is significantly lower in the knobby peridotite zone than in the cumulus or spinifex zones. Turekian (1974) states that cobalt varies directly with magnesium content, however, Pyke's Hill data shows no such correlation. Variation in cobalt concentrations cannot be adequately explained.

5.9 Gold

Gold content in the knobby peridotite zone is 1.98 $\pm$ 1.27 ppb. Analysis by MacRae and Crocket (1977) of two flows at Pyke's Hill indicate gold values of 2.14 and 2.53 ppb in the knobby peridotite zones. Analysis of the different zones within the flows indicate similar gold ranges (1.31 to 3.47 ppb) relative to the knobby peridotite. The distribution of gold is fairly homogeneous with the exception of a 6.63 ppb reading in the (B_2) peridotite zone of one of the flows.

More intensely altered ultramafic rocks near Timmins, Ontario were analyzed by Fyon (1980) showing gold values that concentrated near 4.5 ppb and ranged up to 5 ppb. The combination of different analysis would seem to indicate that there is little migration or removal of gold due to alteration. No pronounced removal of gold with seawater occurs during the cooling of the primitive magma.

Analysis of major elements and trace elements show no clear correlation with gold abundances suggesting that gold acts as a neutral element during magmatic processes (Crocket, 1974). Sulfur analysis using data from both XRF and Leco methods indicate no positive correlation of sulfur with gold.

5.10 Volatiles

No significant variation in volatile content (Loss of ignition, CO_2, S) is evident between different zones within the flow. Since metamorphism is presumably uniform throughout the flows (Arndt et al, 1977) redistribution of volatiles should be insignificant.

CHAPTER 6

Comments on Genesis and Conclusions

6.1 Genesis

The ultramafic flows at Pyke's Hill originated as submarine magmatic eruptions that spread out as low viscosity fluids. During the eruption and spreading phase extrusive lavas probably underwent the type of flowage differentiation demonstrated experimentally by Bhattchaya (1964). The initial suspension contained 10% intratelluric olivine (ie. existing in the magma upon eruption) that was almost instantaneously deposited at the base of the flow (Usselman et al, 1979). The magma underwent fractional crystallization, producing olivine phenocrysts that settled out once the magma had ceased flowing.

Rapid heat loss at the top of the flow produces a thick crust that fractures in polygonal patterns due to contraction. A convective current develops in the seawater above the flow, cycling cool water over the flow to maintain the cooling process. Heat is also conducted into the underlying country rock producing a crust at the base of the flow. The dissipation of heat through the country rock is significantly slower than in the seawater above, thus the advancement of the solid-liquid interface is much slower at the base of the flow than from the top. The development of an upper and lower crust insolates the flow thermally, reducing the rate of cooling.

When the flow is in a static stage, the settling of phenocrysts produce an upper zone devoid of crystals. A steep geothermal gradient develops from the centre of the flow to the upper crust. This gradient initiates quench cooling of the crystal free zone producing blades or needles of olivine that grow down into the underlying liquid (spinifex texture). Spinifex growth is terminated once phenocrysts in the cumulus zone have been reached.

A more gradual geothermal gradient develops from the centre of the flow to the lower crust. The quench cooling initiated in this lower geothermal gradient is not able to form spinifex texture because of the slower rate of cooling and the growth restrictions incurred by cumulus phenocrysts. Since intratelluric crystals consolidate at the base of the flow and cumulus olivine concentrates in the region underlying the spinifex, the intermediate knobby peridotite zone should have the lowest concentration of cumulus crystals.

6.2 Conclusions on Genesis

In a cumulus area containing a lesser quantity of olivine phenocrysts, quench cooling will produce nodules of devitrified glass interstitial to olivine clusters. If this reduced phenocryst area is not present, then knobby peridotite should not form.

The knobby peridotite zone probably best represents the original magma composition. Only minor amounts of cumulus olivine from overlying zones have settled in the knobby peridotite zone making it less contaminated by cumulus olivines and more representative of the original magma composition than other cumulus zones. The spinifex zones is not representative of the original magma because it has been contaminated by seawater during cooling and has lost crystals due to settling of fractionated olivines.

a) Non-Spinifex Flows

Non-spinifex flows may represent lavas further from the magmatic source (Pyke et al, 1973) or may represent flows that were extruded at lower temperatures (Nesbitt, 1971). In either case, the viscosity of the flow is greater than in spinifex bearing flows, thus olivine grains remain suspended throughout the lava. Since the upper portion of the flow contains phenocrysts, spinifex growth is prevented.

6.3 Conclusions

1) All knobby peridotite accumulations are stratabound within the cumulus zones of individual flows and were never crosscut by flow boundaries.
2) Individual knobby protuberances form due to local accumulations of ovoid masses of devitrified glass and associated skeletal clinpyroxene and olivine. This interstitial glass has greater weathering resistance than adjacent olivine concentrations. Extensive breakdown and serpentinization of the olivine crystals may account for the significant weathering of olivine cumulates.
3) Nickel originally contained in silicate form (eg. olivine) is converted during serpentinization to opague mineralogy. The opague minerals

produced are dependent on the amount of sulfur present and the fO_2 environment produced by alteration. The Pyke's Hill assemblage includes heazelwoodite and magnetite. Chromite is a relict mineral being replaced by magnetite.

4) With the exception of enriched Fe_2O_3 and depleated CO, the knobby peridotite zone showed no significant deviation in major or trace element concentrations from other cumulus peridotite zones.

5) The spinifex zone shows enrichment in SiO_2, CaO and Cr with depletion in Al_2O_3 and MgO relative to the cumulus position of the flow. The differences can be attributed to olivine fractionation and gravitational settling of olivine phenocrysts. Other major or trace elements show no significant variation.

6) The volatile content, measured using LOI and CO_2 indicates little deviation between the zones.

7) Gold acts as a neutral element and is found in very low concentrations. (Average 2 ± 1 ppb). These gold values are consistent with gold values in the spinifex and cumulus zones.

6.4 Suggestions For Further Work

1) Microprobe analysis of interstitial glass.
   a) Does the MgO in the devitrified glass compensate for the lack of olivine in the knobby peridotite zone?
   b) Does the interstitial glass best represent the magma composition?

APPENDIX I

MODAL ANALYSIS OF THIN SECTIONS

MODAL ANALYSIS

SAMPLE	PH2	PH3*	PH4	PH5	PH6	PH7*	PH9*	PH10	PH12	PH13*	PH14*	PH15*	PH16*	PH17
OLIVINE	2	7	22	45	16	43	46	45	20	22	48	28	38	35
MAGNETITE	16	11	9	10	5	6	5	10	15	7	9	11	15	13
CHROMITE	1	2	3	4	3	2	2	3	1	3	2	3	2	4
ENSTATITE	-	-	5	-	4	3	3	-	-	1	2	9	-	12
SERPENTINE	72a)	61	35	7	19	6	11	10	15	17	9	10	15	21
PLAGIOCLASE SERICITE	-	-	4	-	-	Tr	-	-	-	-	-	-	-	-
TERMOLITE	-	-	2	4	2	12	3	14	4	7	5	13	5	6
DEVITRIFIED GLASS			25			10	14	7			14	18		2
	b)10%	b)19%		30	b)51				b)45	b)43			25	
AUGITE			5			18	16	11			11	8		7
BRUCITE	-	-	-	-	-	-	-	-	-	-	-	-	-	-

a) Lizardite - 30%
Antigorite - 40%

b) Too Hard to Differentiate

c) Glass Matrix

* Indicates 1000 Point Counts Taken

APPENDIX II

C.I.P.W. NORMALIZATION

C.I.P.W. NORMALIZATION*

	PH1	PH2	PH3	PH4	PH5	PH6	PH7	PH9
CALCITE	0.705	0.546	0.705	0.955	0.500	1.183	0.773	1.046
APATITE	0.046	0.023	-	-	-	-	-	-
ILMENITE	0.266	0.342	0.456	0.645	0.456	0.437	0.570	0.627
ORTHOCLASE	0.059	-	0.355	0.591	0.295	0.177	0.177	0.532
ALBITE	3.723	3.131	3.131	4.823	5.416	3.723	3.808	6.262
ANORTHITE	4.161	0.253	10.414	14.446	9.177	9.370	12.981	13.003
CORUNDUM	0.461	2.248	-	-	-	-	-	-
MAGNETITE	5.423	4.727	5.495	5.959	5.640	5.945	5.756	6.090
FORSTERITE	61.218	57.162	53.675	35.881	56.573	46.830	45.274	42.124
FAYALITE	7.657	6.009	7.274	6.633	7.996	7.364	7.199	7.489
HYPERSTHENE	7.823	18.073	8.723	14.779	2.148	14.937	10.999	10.418
ENSTATITE	7.026	16.500	7.768	12.656	1.904	13.072	9.612	8.971
FERROSILITE	0.797	1.574	0.955	2.123	0.244	1.865	1.387	1.447
DIOPSIDE	-	-	6.886	12.299	8.410	4.147	8.815	11.154

* C.I.P.W. Norms were calculated assuming that the ratio of Fe^{3+} : Fe^{2+} is 1:3

C.I.P.W. NORMALIZATION (Continued)

	PH10	PH11	PH12	PH13	PH14	PH15	PH16	PH17
CALCITE	1.001	0.705	1.001	1.183	0.773	0.864	0.773	0.814
APATITE	-	-	-	-	-	-	-	-
ILMENTITE	0.456	0.665	0.551	0.589	0.532	0.589	0.570	0.499
ORTHOCLASE	0.295	0.650	0.414	0.177	0.473	0.532	0.414	0.453
ALBITE	4.146	6.769	3.469	4.400	3.639	6.769	7.193	4.127
ANORTHITE	9.550	13.794	12.688	12.885	11.150	11.288	11.641	12.415
CORUNDUM	-	-	-	-	-	-	-	-
MAGNETITE	5.539	6.046	5.771	6.017	6.278	6.133	6.119	6.074
FORSTERITE	54.784	35.877	43.551	44.404	44.093	43.733	47.268	47.421
FAYALITE	7.483	6.943	6.930	7.366	7.712	7.735	8.098	7.223
HYPERSTHENE	7.741	12.027	13.230	14.190	12.693	8.809	5.279	12.738
ENSTATITE	6.888	10.230	11.561	12.334	10.955	7.591	4.569	7.744
FERROSILITE	0.854	1.796	1.669	1.856	1.739	1.218	0.710	1.372
DIOPSIDE	6.978	13.217	9.449	4.822	8.470	10.791	12.080	10.643

APPENDIX III

CATION MOLAR PROPORTIONS

(AS PLOTTED ON JENSEN CATION PLOT)

CATION MOLAR PROPORTIONS

(As plotted on Jenson Cation Plot)

Sample No.	AL	MG	FE+TI
PH1	4.69	82.76	12.55
PH2	5.01	84.21	10.79
PH3	7.99	78.87	13.14
PH4	12.84	70.90	16.27
PH5	7.99	78.40	13.61
PH6	7.81	77.30	14.89
PH7	10.46	74.84	14.70
PH9	11.76	72.34	15.90
PH10	7.70	79.06	13.23
PH11	13.37	69.84	16.79
PH12	10.27	74.98	14.75
PH13	10.54	74.23	15.23
PH14	9.28	74.65	16.07
PH15	10.75	73.24	16.01
PH16	10.80	73.65	15.55
PH17	9.17	75.10	15.73

REFERENCES

Arndt, N.T., 1975, Ultramafic rocks of Munro Township and their Volcanic Setting, Unpubl. thesis, University of Toronto, Toronto, Ontario

Arndt, N.T., Naldrett, A.J., Pyke, P.R., 1977, Komatiitic and Iron Rich Tholeittic lavas of Munro Township, Northeastern Ontario, Jour. of Petrology 18, p. 319-369.

Arndt, N.T., Hynes, F.D., Francis, D., 1979, Field characteristics and petrology of Archean and Proterozoic komatiites, Can. Mineral, 17, p. 147-165.

Berry, L.G., 1940, Geology of the Langmuir - Sheraton area, Ontario Dept. Mines Ann. Rept. v49, pt. 4, p. 21.

Battachayi, S., 1967, Scale model experiments on flowage differentiation in sills, in Wylee, P.J., ed, Ultramafic and related rock, New York, John Wiley & Sons, Inc., p. 69-70.

Bowen, N.L., 1956, The Evolution of Igneous rock, Dover Publications Inc., New York, p. 332.

Chamberlain, J.A., 1966, Heazelwoodite and awaruite in serpentinites of the Eastern Townships, Quebec, Can. Mineral, 8, p. 519-522.

Crocket, J.H., Keay, R.R., Hsieh, S., 1968, Determination of some precious metals by neutron activation analysis, J. Radioanal. Chemistry, 1, p. 487-507.

Crocket, J.H., 1974, Gold - Handbook of Geochemistry, Volume 11/4, Springer Verlag, Berlin.

Eckstrand, O.R., 1975, The Dumont Serpentinite, A model for Control of Nickeliferous Opaque mineral assemblages by alteration reactions in Ultramafic Rocks, Econ. Geol. 70, p. 183-201.

Fyon, J.A., 1980, Seawater alteration of early P€ (Archean) Volcanic Rock and exploration criteria for stratiform gold deposits, Porcupine Camp, Abitibi Greenstone Belt, Northeastern Ontario. Unpubl. MSc thesis, McMaster University, Hamilton, Ontario

Goodwin, A.M., and Ridler, R.H., 1970, The Abitibi orogenic belt, p. 1-30 in Symposium of Basins and Geosynclines of Canadian Shield, ed, A.J. Baer, G.S.C. Paper 70-40, p. 265.

Green, D.H., 1975, Genesis of Archean peridotite magmas and constraints of Archean geothermal gradient and tectonics, Geology, 3, p. 15-18.

Green, D.H., and Ringwood, A.E., 1967, An experimental investigation of the gabbro to eclogite transformation and its petrological application, Geochem. Cosmochim. Acta, 31, p. 767-833.

Grubb, P.L.C., 1962, Serpentinization and crystolite formation in the Matheson ultrabasic belt, N. Ontario, Econ. Geol., 57, p. 1228-1246.

Gunn, B.M., 1971, Trace Element partition during olivine fractionation of Hawaiian Basalts. Chem. Geol., 8, p. 1-30.

Hatch, F.H., 1926, Petrology of Igneous Rocks, The MacMillan Company, London.

Hawley, J.E., 1962, The Sudbury ores, their mineralogy and origin: Can. Mineral, 7, p. 1-207.

Hutchinson, C.S., 1974, Laboratory handbook of petrographic techniques, John Wiley and Sons, New York, p. 264-332.

Jenson, L.S., 1976, A new Cation plot for classifying subalkaline volcanic rocks, Ministry of Natural Resources, Misc. Paper 66.

Jolly, W.J., 1980, Development of degradation of Archean lavas, Abitibi Area, Canada, in light element chemistry, Jour. of Petrology, 21, p. 323-363.

Kerr, P.F., 1977, Optical Mineralogy, Second Edition, McGraw Hill Inc., Toronto, p. 305.

MacRae, N.D., 1963, Petrology of the Centre Hill Complex, unpublished M.Sc. thesis, McMaster University, p. 120.

MacRae, N.D., 1965, Petrology and geochemistry of ultramafic-gabbroic intrusions in the Abitibi area, Ontario, Unpubl. PH.D., thesis, McMaster University, Hamilton, Ontario, p. 163.

MacRae, N.D., 1969, Ultramafic intrusions of the Abitibi area, Ontario, Can. Jour. of Earth Sciences, 6, p. 281-303.

MacRae, W.E., 1981, unpublished data, McMaster University, Hamilton, Ont.

MacRae, W.E. and Crockett, J. H., 1977, The distribution of gold and some platinum group elements in selected komatiitic ultramafic volcanics from Munro Township, Ontario. Geol. Assoc. Can. Mineral. Assoc. Can. Program Abst. 2:34.

Marchand, M., 1973, Determination of Rb, Sr, and Rb/Sr by X.R.F. Tech. Memo 73-2, Dept. of Geology, McMaster University, Hamilton, Ontario Canada.

Mattison, G.D., 1973, C.I.P.W. Norm Program, Dept. of Geochemistry and Mineralogy, Pennsylvania State University.

Naldrett, A.J., 1964, Ultrabasic Rocks of the Porcupine and related nickel deposits, Unpubl. PH.D. thesis, Queen's University, Kingston, Ont.

Naldrett, A.J. and Mason, G.D., 1968, Contrasting Archean Ultramafic igneous bodies in Dundonald and Clergue Townships, Can. Jour. Earth Sciences, 5, p. 111-143.

Naldrett, A.J. and Cabri, L.J., 1976, Ultramafic and related Mafic rocks: Their classification and genesis with special reference to the concentration of nickel sulfides and platinum group elements. Econ. Geol. 71, p. 1131-1159.

Naldrett, A.J., 1973, Nickel Sulfide Deposits - Their classification and genesis, with special emphasis on deposits of Volcanic Assoc. Can. Inst., Min. Metal, Trans, Vol. 76, p. 183 - 201.

Nesbitt, R.W., 1971, Skeletal crystal forms in the Ultramafic rocks of the Yilgarn Block, Western Australia, Evidence for an Archean ultramafic liquid, Geol. Soc. Aust. Spec. Publ., 3, p. 331-347.

Nickel, E.H., 1959, The occurrance of native nickel iron in the Serpentinized rock of the Eastern Townships of Quebec, Can. Mineral, 5, p. 307-319.

Pyke, D.R., Naldrett, A.J., Eckstrand, O.R., 1973, Archean ultramafic flows in Munro Township, Ontario, Geol. Soc. of Amer. Bull. 84, p. 995-978.

Satterley, J., 1951, Geology of Munro Township, Ont. Dept. Mines, vol. LX, pt. VIII.

Short, A.J., 1955, Microscopic determination of the ore minerals, Geol. Survey Bulletin 914, p. 1-140.

Turekian, K.K., 1974, Cobalt-Handbook of Geochemistry, Vol. 11/3, Springer Verlag, Berlin.

Usselman, T.M., Hodge, D.S.,; Naldrett, A.J.; Campbell, I.H.; 1979, Physical Constraints on the Characteristics of Nickel - Sulfide ore in Ultramafic Lavas, Can. Mineral., 17, p. 361-372.

Uytenbogaart, R. and Burke, E.A.J., 1973, Tables for microscopic identification of ore minerals, Elevier Scientific Publishing Company, second edition, New York.

Viljoen, M.J. and Viljoen, R.R., 1969, Evidence for the existence of a mobile extrusive peridotite magma from the Komati Formation of the Onverwact Group, Geol. Soc. of S. Africa, Spec. Publ. 2, Upper Mantle Project, p. 87-112.

Vogt, J.H.L., 1926, Magmas and Igneous ore deposits, Economic Geology, 21, p. 207-234.

Winkler, H.G.F., 1980, Petrogenesis of Metamorphic Rocks, Fifth Edition, Springler Verlag, New York.

Woodal, R. and Travis, G.A., 1969, The Kambalda Nickel Deposits, Western Australia, Publ. 9th Commonwealth Min. and Met. Congress, Paper 26, p. 17.